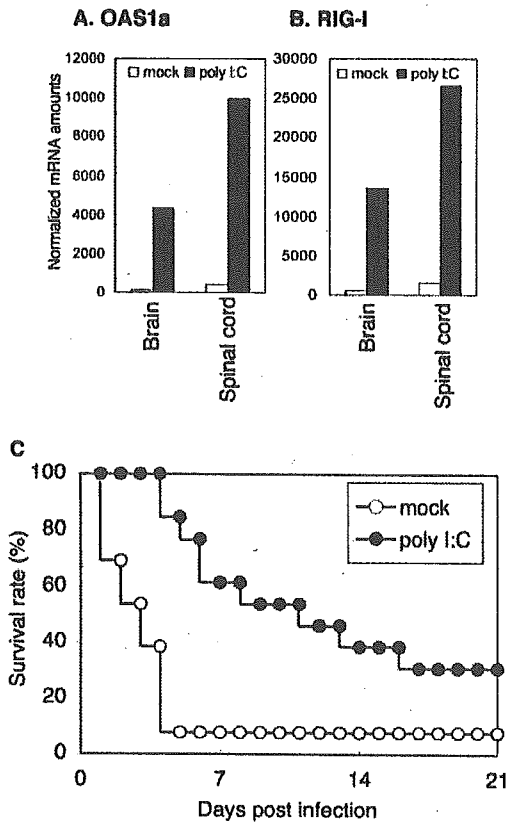

FIG. 7. Induction of mRNAs for OAS1a (A) and RIG-I (B) after poly(I:C) treatment. PVR-transgenic mice was administered poly(I:C) (solid bars) or mock treated (open bars). RNA was prepared from the mice 1 day after administration. The amounts of RNA were determined by real-time quantitative PCR. (C) Survival of infected mice. PVR-transgenic mice administered poly(I:C) (solid circles) or mock treated (open circles) (13 mice each) were challenged intracerebrally with 10^4 PFU of poliovirus. Mice were observed for 3 weeks. The survival rate of poly(I:C)-treated mice was significantly higher than that of mock-treated mice ($P < 0.05$, log-rank test).

(10^4 PFU) by the same route. The survival of the mice is shown in Fig. 7C. Mock-treated PVR-transgenic mice died at 2 to 6 days p.i., with a survival rate of 7.7%. After poly(I:C) treatment, mice died at 4 to 16 days p.i., increasing the survival rate to 30.8%. The clinical symptoms observed in the poly(I:C)-treated PVR-transgenic mice were almost the same as those observed in mock-treated mice, suggesting the same pathology. The results indicate that the poly(I:C)-treated mice survived longer than mock-treated mice, with the survival rate of poly(I:C)-treated mice being higher than that of mock-treated mice ($P < 0.05$, log rank test). These data suggest that the antiviral state induced by treatment with poly(I:C) was effective in preventing poliovirus replication in the central nervous system.

DISCUSSION

IFN system is a host factor that inhibits poliovirus replication. Picornaviruses are sensitive to IFNs. However, little is known about the role of alpha/beta IFN in the pathogenesis of poliovirus in vivo. We have shown the importance of the IFN response in poliovirus infection in vivo with a transgenic mouse expressing human PVR. In the PVR-transgenic mice, poliovirus replicates and produces severe lesions in the brain and spinal cord, while other tissues did not show severe pathological changes.

It would be reasonable to assume that some host factors required for poliovirus replication are lacking in the nontarget cells and tissues. PVR was thought to be such a determinant (13). However, previous studies revealed that many nontarget tissues expressed PVR (18, 21, 24, 31, 32). It is therefore impossible to explain poliovirus tissue tropism solely by the presence of PVR. Gromeier et al. (11) and Yanagiya et al. (46) proposed a hypothetical mechanism called the internal ribosome entry site (IRES)-dependent mechanism to explain the tissue tropism of viruses. The IRES controls the efficiency of protein synthesis in some viruses. Chimeric viruses containing the IRES of human rhinovirus and hepatitis C virus instead of the poliovirus IRES do not replicate in the central nervous system. Therefore, the poliovirus IRES confers the ability to replicate in neurons on the chimeric virus, while the IRESs of human rhinovirus and hepatitis C virus do not. It is possible that the poliovirus IRES, particularly in virulent strains, is designed to exhibit full activity in neurons. In this hypothesis, host factors related to poliovirus IRES function should be restricted to neurons. However, poliovirus can replicate in cultured cells of nonneural origin. This hypothesis does not completely explain why poliovirus does not replicate efficiently in nontarget tissues in vivo.

It is also possible to assume that some host factors that inhibit poliovirus replication are present in the nontarget tissues. The liver, spleen, and pancreas were spared severe poliovirus infection only when the IFN system was functional. These data demonstrate that the IFN system is one of the major factors that confers resistance against poliovirus infection. Limitation of poliovirus tissue tropism is achieved by inhibition of poliovirus replication by the IFN system in nontarget tissues. An altered tissue distribution of viral replication was observed in mice deficient in the *Ifnar* gene or in mice deficient in the signal transducer and activator of transcription 1 (*Stat-1*) gene infected with viruses other than poliovirus (9, 10, 28, 34, 44). In these animals, virus replication was observed in tissues that were normally considered nontarget tissues. Therefore, it is a general principle that the tissue tropism of viruses is determined, at least in part, by an IFN-dependent mechanism.

Unequal IFN response selectively inhibits poliovirus replication in nontarget tissues. In cultured cells, encephalomyocarditis virus replication occurs rapidly within 6 h, and the infected cells are usually destroyed by lytic replication of virus before they produce IFNs. However, constitutive expression of OAS or protein kinase R (7, 8, 25), which are effectors of antiviral activity, and expression of RIG-I (48), a regulator of IFN induction, inhibited viral replication. It is very likely that the same mechanism operates during poliovirus infection.

We determined the expression of ISGs in the tissues. The distribution of ISG mRNAs in the noninfected mice was not equal among tissues. They were expressed in the nontarget tissues more abundantly than in the target tissues (Fig. 5). These existing ISG products may help restrict virus replication and spread in the nontarget tissues during the initiation of infection in vivo. In PVR-transgenic/*Ifnar* knockout mice, the

expression levels of mRNAs for ISGs were greatly reduced. The mRNAs for OASs were detected only in the intestine and thymus (data not shown). This is also consistent with the result of Ueda et al. (43), which showed that OAS expression in most tissues was reduced in p48 (IRF-9)-deficient mice. This result suggests that ISG expression in most of the tissues, even in the noninfected state, is mainly dependent on the IFNAR-dependent pathway. It also suggests that these tissues were continuously exposed to IFN stimulation at low levels (43). Visceral tissues such as the intestine and lungs are continuously at risk of exposure to pathogens. These tissues may be programmed to respond readily to viral infection. Alternatively, they are constantly stimulated by nonpathogenic microorganisms present in the body and thus are already primed.

Furthermore, the IFN response after poliovirus infection was also different among tissues. High-level response was observed in the spleen but was not observed in the spinal cord. This suggests that the IFN response profile may differ depending on the cells and tissues. Since RIG-I and MDA-5/helicard are also IFN inducible (17, 48), they also existed more abundantly in the nontarget tissues (Fig. 6), like other ISGs (Fig. 5). Some of the important regulators of the IFN response, such as IRF-7 and IRF-9, are also IFN inducible. The cells that are primed even at low levels of IFNs may be equipped with all the machinery necessary for the IFN response. Thus, the nontarget tissues may be ready to respond to viral infection. Unequal distribution of the regulators of the IFN response is again consistent with the idea that poliovirus replication is selectively inhibited in nontarget tissues.

On the contrary, neurons in the brainstem and spinal cord could not induce a sufficient antiviral state after poliovirus infection. However, pretreatment with poly(I:C) increased the survival of PVR-transgenic mice against poliovirus challenge (Fig. 7). This suggests that neurons also became resistant to poliovirus infection as long as they were treated. It is therefore possible that the status of ISG expression in the early phase of infection is critical in determining the fate of infected cells and an unequal IFN response may be one of the reasons for the differential susceptibility of cells and tissues to poliovirus. Although the IFN response was not equal in PVR-transgenic mice, both the basal expression of ISGs and induction of ISGs after poliovirus infection are equally null in PVR-transgenic/*Ifnar* knockout mice. Without these unequal protective responses, replication of poliovirus was observed in PVR-transgenic/*Ifnar* knockout mice in the nontarget tissues as well.

Incidence of paralytic disease is influenced by the IFN response. In a natural poliovirus infection, less than 1% of infected individuals develop paralytic disease, and virus clearance occurs in most persons with asymptomatic or mild infections (4, 23, 35). Viremia is observed only transiently in experimentally infected chimpanzees and monkeys, with titers of less than 10^5 tissue culture infective doses per ml with virulent strains (3, 5). Viremia was not observed in a chimpanzee and a human volunteer administered attenuated vaccine strains (35). Thus, viremia titers seem to correlate with central nervous system invasion in primates.

Our data showed that viral replication in visceral tissues is inhibited by the IFN response in PVR-transgenic mice. Poliovirus can enter the central nervous system, penetrating the blood-brain barrier. This pathway is considered the main pathway of poliovirus entry into the central nervous system in the PVR-transgenic mice after poliovirus infection via peripheral routes (47). Inhibition thus results in reduction of the virus titer in the blood and reduction of the chance of virus entry into the central nervous system. In contrast, PVR-transgenic/*Ifnar* knockout mice showed viremia with a very high titer and a high incidence of paralytic disease. It is therefore possible to speculate that the low incidence of paralytic poliomyelitis in humans is also a result of inhibition of poliovirus replication in nonneural tissues by the host IFN response, although we have no experimental evidence on humans. Paralytic poliomyelitis may occur when the alpha/beta IFN response does not work sufficiently in patients with certain conditions. Individuals who have a defect(s) in a gene(s) that contributes to the IFN response would be more susceptible to paralytic poliomyelitis.

Conclusion. The tissue tropism and pathogenesis of viruses are determined by a combination of several factors. In the case of poliovirus infection, poliovirus replication sites are primarily determined by the presence of the receptor, with the capture and entry of the virus into the cells supported by the PVR. Cells expressing PVR at high levels may be favored for poliovirus infection (20). Thus, the tropism of poliovirus may be dependent on the amount of PVR. After virus entry into cells, efficient replication of poliovirus may be dependent on the milieu of infected cells. If the environment is optimal for RNA and viral protein synthesis, a large number of viral particles will be produced per cell. If antiviral activities, such as the IFN response, are sufficiently high, virus replication will be inhibited. Thus, the fate of infected cells is determined by the balance of the replicating capacity of poliovirus and the antiviral activity of the host. Visceral tissues will then fail to serve as a massive factory of poliovirus, and the chance of viral entry into the central nervous system is greatly reduced.

If the virus enters the central nervous system, virulent poliovirus strains can replicate in neurons, where the antiviral defense is not sufficiently ready, and the patient develops paralytic disease. Therefore, the innate antiviral defense is an important determinant of tissue tropism and pathogenicity of poliovirus. It is of interest to investigate if the alpha/beta IFN response also contributes to selective poliovirus infection in the motor neurons in the central nervous system or to infection in the gastrointestinal tract. These questions will be elucidated in future studies. In the case of other viruses, situations such as distribution of the receptor molecule, replication capacity in each tissue, and resistance to the IFN system may differ from those of poliovirus. It therefore seems likely that each virus displays a distinct disease pattern unique to that particular virus.

ACKNOWLEDGMENTS

We thank Masayoshi Kohase, Seii Ohka, Akio Nomoto, Hitoshi Horie, Shinobu Abe, Bunshichi Shimizu, Sou Hashizume, Michiaki Masuda, Masahiko Takada, Eckard Wimmer, and Yoshiyuki Nagai for providing materials, technical assistance, and helpful discussion.

This work was supported in part by a Grant-in-Aid for Scientific Research from the Japanese Ministry of Education, Culture, Sports, Science, and Technology and by a Grant-in-Aid for Research on Emerging and Re-emerging Infectious Diseases from the Japanese Ministry of Health, Labour and Welfare.

REFERENCES

1. **Asada-Kubota, M., T. Ueda, M. Shimada, K. Takeda, and T. Sokawa.** 1995. Distribution of immunoreactive 2′, 5′-oligoadenylate synthetase in mouse digestive tract. J. Interferon Cytokine Res. **15:**863–867.
2. **Bodian, D.** 1949. Histopathologic basis of clinical findings in poliomyelitis. Am. J. Med. **6:**563–578.
3. **Bodian, D.** 1954. Viremia in experimental poliomyelitis. I. General aspects of infection after intravascular inoculation with strains of high and of low invasiveness. Am. J. Hyg. **60:**339–357.
4. **Bodian, D.** 1955. Emerging concept of poliomyelitis infection. Science **12:** 105–108.
5. **Bodian, D.** 1956. Poliovirus in chimpanzee tissues after virus feeding. Am. J. Hyg. **64:**181–197.
6. **Bodian, D., and H. A. Howe.** 1940. An experimental study of the role of neurones in the dissemination of poliomyelitis virus in the nervous system. Brain **63:**135–167.
7. **Chebath, J., P. Benech, M. Revel, and M. Vigneron.** 1987. Constitutive expression of (2′-5′) oligo A synthetase confers resistance to picornavirus infection. Nature **330:**587–588.
8. **Coccia, E. M., G. Romeo, A. Nissim, G. Marzaili, R. Albertini, E. Affabris, A. Battistini, G. Fiorucci, R. Orsatti, G. B. Rossi, and J. Chebath.** 1990. A full-length murine 2-5A synthetase cDNA transfected in NIH-3T3 cells impairs EMCV but not VSV replication. Virology **179:**228–233.
9. **Fiette, L., C. Aubert, U. Mueller, S. Huang, M. Aguet, and M. Brahic, and J.-F. Bureau.** 1995. Theiler's virus infection of 129Sv mice that lack the interferon α/β or interferon γ receptors. J. Exp. Med. **181:**2069–2076.
10. **Garcia-Sastre, A., R. K. Durbin, H. Zheng, P. Palese, R. Gertner, D. E. Levy, and J. E. Durbin.** 1998. The role of interferon in influenza virus tissue tropism. J. Virol. **72:**8550–8558.
11. **Gromeier, M., L. Alexander, and E. Wimmer.** 1996. Internal ribosomal entry site substitution eliminates neurovirulence in intergeneric poliovirus recombinants. Proc. Natl. Acad. Sci. USA **93:**2370–2375.
12. **Henkel, E., S. Morich, and R. Henkel.** 1984. 2-chloro-4-nitrophenyl-β-D-maltoheptaoxide: A new substrate for the determination of α-amylase in serum and urine. J. Clin. Chem. Clin. Biochem. **22:**489–495.
13. **Holland, J. J.** 1961. Receptor affinities as major determinants of enterovirus tissue tropisms in humans. Virology **15:**312–326.
14. **Ida-Hosonuma, M., T. Iwasaki, C. Taya, Y. Sato, J. Li, N. Nagata, H. Yonekawa, and S. Koike.** 2002. Comparison of neuropathogenicity of poliovirus in two transgenic mouse strains expressing human poliovirus receptor with different distribution patterns. J. Gen. Virol. **83:**1095–1105.
15. **Iwasaki, A., R. Welker, S. Mueller, M. Linehan, A. Nomoto, and E. Wimmer.** 2002. Immunofluorescence analysis of poliovirus receptor expression in Peyer's patches of humans, primates, and CD155 transgenic mice: implications for poliovirus infection. J. Infect. Dis. **186:**585–592.
16. **Kakuta, S., S. Shibata, and Y. Iwakura.** 2002. Genomic structure of the mouse 2′, 5′-oligoadenylate synthetase gene family. J. Interferon Cytokine Res. **22:**981–993.
17. **Kang, D.-C., R. V. Gopalkrishnan, Q. Wu, E. Jankowsky, A. M. Pyle, and P. B. Fisher.** 2002. mda-5: An intereferon-inducible putative RNA helicase with double-stranded RNA-dependent ATPase activity and melanoma growth-suppressive properties. Proc. Natl. Acad. Sci. USA **99:**637–642.
18. **Koike, S., H. Horie, I. Ise, A. Okitsu, M. Yoshida, N. Iizuka, K. Takeuchi, T. Takegami, and A. Nomoto.** 1990. The poliovirus receptor protein is produced both as membrane-bound and secreted forms. EMBO J. **9:**3217–3224.
19. **Koike, S., I. Ise, Y. Sato, H. Yonekawa, O. Gotoh, and A. Nomoto.** 1992. A second gene for the African green monkey poliovirus receptor that has no putative N-glycosylation site in the functional N-terminal immunoglobulin-like domain. J. Virol. **66:**7059–7066.
20. **Koike, S., C. Taya, J. Aoki, Y. Matsuda, I. Ise, H. Takeda, T. Matsuzaki, H. Amanuma, H. Yonekawa, and A. Nomoto.** 1994. Characterization of three different transgenic mouse lines that carry human poliovirus receptor gene –influence of the transgene expression on pathogenesis. Arch. Virol. **139:** 351–363.
21. **Koike, S., C. Taya, T. Kurata, S. Abe, I. Ise, H. Yonekawa, and A. Nomoto.** 1991. Transgenic mice susceptible to poliovirus. Proc. Natl. Acad. Sci. USA **88:**951–955.
22. **Mashimo, T., P. Glasser, M. Lucas, D. Simon-Chazottes, P. E. Ceccaldi, X. Montagutelli, P. Despres, and J.-L. Guénet.** 2003. Structural and functional genomics and evolutionary relationship in the cluster of genes encoding murine 2′,5′-oligoadenylate synthetases. Genomics **82:**537–552.
23. **Melnick, J. L.** 1996. Enteroviruses: polioviruses, coxsackieviruses, echoviruses, and newer enteroviruses, p. 655–712. *In* B. N. Fields, D. M. Knipe, and P. M. Howley (ed.) Fields virology, 3rd ed. Lippincott-Raven, Philadelphia, Pa.
24. **Mendelson, C. L., E. Wimmer, and V. R. Racaniello.** 1989. Cellular receptor for poliovirus: molecular cloning, nucleotide sequence, and expression of a new member of the immunoglobulin superfamily. Cell **56:**855–865.
25. **Meurs, E. F., Y. Watanabe, S. Kadereit, G. N. Barber, M. G. Katze, K. Chong, B. R. Williams, and A. G. Hovanessian.** 1992. Constitutive expression of human double-stranded RNA-activated p68 kinase in murine cells mediates phosphorylation of eukaryotic initiation factor 2 and partial resistance to encephalomyocarditis virus growth. J. Virol. **66:**5805–5814.
26. **Müller, U., U. Stainhoff, L. F. Reis, S. Hemmi, J. Pavlovic, R. M. Zinkernagel, and M. Aguet.** 1994. Functional role of type I and II interferons in antiviral defense. Science **264:**1918–1921.
27. **Munoz, A., and L. Carrasco.** 1984. Action of human lymphoblastoid interferon on HeLa cells infected with RNA-containing animal viruses. J. Gen. Virol. **65:**377–390.
28. **Mrkic, B., J. Pavlovic, J., T. Ruelicke, P. Volpe, C. J. Buchholz, D. Hourcade, J. P. Atkinson, A. Aguzzi, and R. Cattaneo.** 1998. Measles virus spread and pathogenesis in genetically modified mice. J. Virol. **72:**7420–7427.
29. **Nomoto, A., S. Koike, and J. Aoki.** 1994. Tissue tropism and species specificity of poliovirus infection. Trends Microbiol. **2:**47–51.
30. **Perelygan, A. A., S. V. Scherbik, I. B. Zhulin, B. M. Stockman, Y. Li, and M. A. Brinton.** 2002. Positional cloning of the murine flavivirus resistance gene. Proc. Natl. Acad. Sci. USA **99:**9322–9327.
31. **Ren, R., F. Constantini, E. J. Gorgacz, J. J. Lee, and V. R. Racaniello.** 1990. Transgenic mice expressing a human poliovirus receptor: a new model for poliomyelitis. Cell **63:**353–362.
32. **Ren, R., and V. R. Racaniello.** 1992. Human poliovirus receptor gene expression and poliovirus tissue tropism in transgenic mice. J. Virol. **66:**296–304.
33. **Rueckert, R.** 1996. Picornaviridae: the viruses and their replication. p. 609–654. *In* B. N. Fields, D. M. Knipe, and P. M. Howley (ed.) Fields virology, 3rd ed. Lippincott-Raven, Philadelphia, Pa.
34. **Ryman, K., W. B. Klimstra, K. B. Nguyen, C. A. Biron, and R. E. Johnston.** 2000. Alpha/beta interferon protects adult mice from fatal Sindbis virus infection and is an important determinant of cell and tissue tropism. J. Virol. **74:**3366–3378.
35. **Sabin, A.** 1956. Pathogenesis of poliomyelitis: reappraisal in light of the new data. Science **123:**1151–1157.
36. **Samuel, C. E.** 1991. Antiviral actions of interferon. Interferon-regulated cellular proteins and their surprisingly selective antiviral activities. Virology **183:**1–11.
37. **Sato, M., H. Suemori, N. Hata, M. Asargiri, K. Ogasawara, K. Nakao, T. Nakaya, M. Katsuki, S. Noguchi, N. Tanaka, and T. Taniguchi.** 2000. Distinct and essential roles of transcription factors IRF-3 and IRF-7 in response to viruses for IFN-α/β gene induction. Immunity **13:**539–548.
38. **Schneider-Schaulies, J.** 2000. Cellular receptors for viruses: link to tropism and pathogenesis. J. Gen. Virol. **81:**1413–1429.
39. **Sen, G. C., and P. Lengyel.** 1992. The interferon system. A bird's eye view of its biochemistry. J. Biol. Chem. **267:**5017–5020.
40. **Shiroki, K., H. Kato, S. Koike, K. Odaka, and A. Nomoto.** 1993. Temperature-sensitive mouse cell factors for strand-specific initiation of poliovirus RNA synthesis. J. Virol. **67:**3989–3991.
41. **Stark, G. R., I. M. Kerr, B. R. G. Williams, R. H. Silverman, and R. D. Schriber.** 1998. How cells respond to interferons. Annu. Rev. Biochem. **67:**227–264.
42. **Tagawa, Y., K. Sekikawa, and Y. Iwakura.** 1997. Suppression of concanavalin A-induced hepatitis in IFN-gamma$^{-/-}$ mice, but not in TNF-alpha$^{-/-}$ mice: role for IFN-gamma in activating apoptosis of hepatocytes. J. Immunol. **159:**1418–1428.
43. **Ueda, T., R. Tatsumi, N. Tanaka, M. Asada-Kubota, K. Hamada, S. Noguchi, T. Taniguchi, and Y. Sokawa.** 1998. Production of immunoreactive 2′,5′-oligoadenylate synthetase in p48-deficient mice. J. Interferon Cytokine Res. **18:**181–185.
44. **Wessely, R., K. Klingel, K. U. Knowlton, and R. Kandolf.** 2001. Cardioselective infection with coxsackievirus B3 requires intact type 1 interferon signaling: implications for mortality and early viral replication. Circulation **103:**765–771.
45. **World Health Organization.** 1990. Manual for the virological investigation of poliomyelitis. World Health Organization, Expanded Programme on Immunization and Division of Communicable Diseases. W.H.O. Publication no. W.H.O./EPI/CDS/POLIO/ 90.1. World Health Organization, Geneva, Switzerland.
46. **Yanagiya, A., S. Ohka, N. Hashida, M. Okamura, C. Taya, N. Kamoshita, K. Iwasaki, Y. Sasaki, H. Yonekawa, and A. Nomoto.** 2003. Tissue-specific replicating capacity of a chimeric poliovirus that carries the internal ribosome entry site of hepatitis C virus in a new mouse model transgenic for the human poliovirus receptor. J. Virol. **77:**10479–10487.
47. **Yang, W. X., T. Terasaki, K. Shiroki, S. Ohka, J. Aoki, S. Tanabe, T. Nomura, E. Terada, Y. Sugiyama, and A. Nomoto.** 1997. Efficient delivery of circulating poliovirus to the central nervous system independently of poliovirus receptor. Virology **17:**421–428.
48. **Yoneyama, M., M. Kikuchi, T. Natsukawa, N. Shinobu, T. Imaizumi, M. Miyagishi, K. Taira, S. Akira, and T. Fujita.** 2004. The RNA helicase RIG-I has an essential function in double-stranded RNA-induced innate antiviral responses. Nat. Immunol. **5:**730–737.
49. **Zhou, A., J. Paranjape, T. L. Brown, H. Nie, S. Naik, B. Dong, A. Chang, B. Trapp, R. Fairchild, C. Colmenares, and R. H. Silverman.** 1997. Interferon action and apoptosis are defective in mice devoid of 2′,5′-oliogoadenylate-dependent RNase L. EMBO J. **16:**6355–6363.

Behavioral/Systems/Cognitive

Organization of Multisynaptic Inputs from Prefrontal Cortex to Primary Motor Cortex as Revealed by Retrograde Transneuronal Transport of Rabies Virus

Shigehiro Miyachi,[1,2] Xiaofeng Lu,[3] Satoshi Inoue,[4] Takuya Iwasaki,[5] Satoshi Koike,[1] Atsushi Nambu,[6] and Masahiko Takada[1,2]

[1]Tokyo Metropolitan Institute for Neuroscience, Fuchu, Tokyo 183-8526, Japan, [2]Core Research for Evolutional Science and Technology, Japan Science and Technology Agency, Kawaguchi 332-0012, Japan, [3]Department of Physiology, Juntendo University School of Medicine, Tokyo 113-8421, Japan, [4]National Institute of Infectious Diseases, Tokyo 162-8640, Japan, [5]Institute of Tropical Medicine, Nagasaki University, Nagasaki 852-8523, Japan, and [6]National Institute for Physiological Sciences, Okazaki 444-8585, Japan

The organization of multisynaptic projections from the prefrontal cortex to the primary motor cortex (MI) was examined in macaque monkeys by retrograde transneuronal transport of rabies virus. In the first series of experiments, the virus was injected into the MI forelimb region, and the time-dependent distribution patterns of transsynaptic labeling were analyzed in the frontal lobe with various survivals (2–4 d). Two days after the viral injection, neuronal labeling emerged in the caudal aspects of the nonprimary motor-related areas that are known to project to the MI directly. At the same time, the motor thalamus contained labeled neurons. On the third day, cortical labeling extended into the rostral motor-related areas and, also, prearcuate area 8. Moreover, a number of labeled neurons were located in the internal pallidum and the cerebellar nuclei. At the 4 d postinjection period, neuronal labeling occurred widely in prefrontal areas as well as in the putamen and the cerebellar cortex. In the second series of experiments, the viral injection was made into the MI hindlimb region, and the distribution pattern of prefrontal labeling on the fourth day was compared with that in the forelimb-injection case. The labeled neurons in each prefrontal area were much fewer in the hindlimb-injection case than in the forelimb-injection case. Whereas ventral area 46 was most densely labeled from the forelimb region, only sparse labeling from the hindlimb region was observed in this prefrontal area. The present results suggest the importance of ventral area 46 in the cognitive control of forelimb movements.

Key words: prefrontal cortex; primary motor cortex; cortical motor-related areas; somatotopy; basal ganglia; cerebellum

Introduction

The frontal lobe plays crucial roles in the execution and control of various motor behaviors in humans and nonhuman primates. The primary motor cortex (MI), lying in the caudalmost portion of the lobe, has massive projections to the spinal cord in a strict somatotopic manner (He et al., 1993; Galea and Darian-Smith, 1994; Dum and Strick, 1996). This implies the involvement of the MI in the precise control of somatic movements (Georgopoulos et al., 1982; Kakei et al., 1999). In the primate MI, forelimb representation occupies a large sector in the precentral gyrus, thus reflecting the importance of forelimb movements compared with the movements of other body parts. On the other hand, located at the rostral pole of the frontal lobe is the prefrontal cortex that consists of multiple, anatomically distinct areas. These prefrontal areas receive inputs from the parietal association, temporal association, and limbic-related cortical areas (Barbas and Mesulam, 1985; Barbas, 1988; Pandya and Yeterian, 1990; Carmichael and Price, 1995a) and, in turn, send outputs to the frontal motor-related areas (Barbas and Pandya, 1987; Luppino et al., 1993; Lu et al., 1994). It has been proposed that individual areas of the prefrontal cortex play differential roles in the control of voluntary actions according to distinct types of sensory and emotional information. For example, the dorsolateral prefrontal cortex has been implicated in motor selection based on visual information (Wilson et al., 1993; Sakagami and Tsutsui, 1999), whereas the medial prefrontal cortex seems to have certain roles in reward- or context-dependent motor selection (Paus, 2001; Matsumoto et al., 2003). The orbitofrontal cortex is suggested to participate in the reward-dependent control of motor behaviors (Tremblay and Schultz, 1999; Hikosaka and Watanabe, 2000). However, the somatotopic delineation of these prefrontal areas remains unknown. Which prefrontal areas are more strongly involved in motor actions involving the forelimb? So far, it has been difficult to elucidate the pattern of somatotopic representations in the prefrontal cortex. One possible reason is that body part movements cannot be evoked by electrical stimulation in the prefrontal cortex, nor can responses to somatosensory stimuli be elicited

Received May 12, 2004; revised Dec. 7, 2004; accepted Dec. 10, 2004.

This work was supported by Grants-in-Aid for Scientific Research (B) and for Scientific Research on Priority Areas from the Ministry of Education, Culture, Sports, Science and Technology of Japan. We are grateful to Etsuko Mine for technical assistance.

Correspondence should be addressed to Dr. Shigehiro Miyachi, Department of System Neuroscience, Tokyo Metropolitan Institute for Neuroscience, Tokyo Metropolitan Organization for Medical Research, 2-6 Musashidai, Fuchu, Tokyo 183-8526, Japan. E-mail: miyachi@tmin.ac.jp.

DOI:10.1523/JNEUROSCI.4186-04.2005

 0270-6474/05/252547-10$15.00/0

in the prefrontal cortex. In addition, neuronal linkage between the prefrontal cortex and the MI is not well understood, because these two structures are interconnected indirectly by way of nonprimary motor-related areas. To address the issue on the somatotopic aspect of the prefrontal cortex in motor control, it is necessary to analyze the multisynaptic connections between the prefrontal cortex and the MI. For this purpose, transneuronal transport of a neurotropic virus is a useful tool. Rabies virus is known to label neurons through synapses in the retrograde direction (Ugolini, 1995; Kelly and Strick, 2000). In the present study, the virus was injected into forelimb representation of the monkey MI, and the time-dependent distributions of transsynaptic labeling were examined in the frontal lobe with varying survivals (2–4 d). The viral injection was further made into hindlimb representation of the MI, and the pattern of prefrontal labeling was compared with that in the forelimb-injection case.

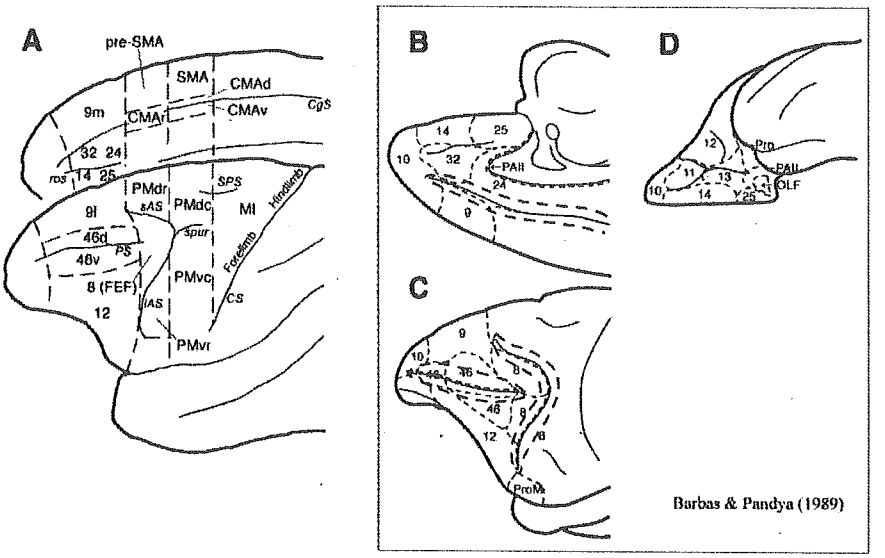

Figure 1. Parcellation of the macaque frontal cortex. *A*, Classification of the prefrontal and motor-related areas used in the present study. *B–D*, Classification of Barbas and Pandya [(1989), their Fig. 2*A–C*, reprinted with permission]. CgS, Cingulate sulcus; CS, central sulcus; iAS, inferior limb of the arcuate sulcus; OLF, olfactory cortex; PAll, limbic periallocortex; Pro, proisocortex; ProM, rostral portion of the ventral premotor cortex; PS, principal sulcus; ros, rostral sulcus; sAS, superior limb of the arcuate sulcus; SPS, superior precentral sulcus; spur, spur of the arcuate sulcus; 8, area 8; 9l, lateral area 9; 9m, medial area 9; 46d, dorsal area 46; 46v, ventral area 46. Numbers correspond to the area numbers defined by Barbas and Pandya (1989).

Materials and Methods

Experimental animals. Ten macaque monkeys (six Japanese and four rhesus monkeys) of either sex weighing 5.5–14 kg were used in this study (see Table 1). Throughout the experimental sessions, the monkeys were kept in individual cages placed inside a special safety cabinet. Food and water were available *ad libitum* in each cage. The experimental protocol was approved by the Animal Care and Use Committee of the Tokyo Metropolitan Institute for Neuroscience (Fuchu, Tokyo, Japan), and all experiments were conducted according to the Tokyo Metropolitan Institute for Neuroscience *Guidelines for the Care and Use of Animals* (2000).

Virus. A stock virus suspension of the challenge-virus-standard (CVS-11) strain was prepared by using mouse neuroblastoma cells of A/J (H-2a) as described previously (Smith et al., 1996). This rabies strain was the same as introduced by Ugolini (1995) and Kelly and Strick (2000) to demonstrate specific retrograde transneuronal transport of the virus. The titer of the stock virus suspension was 1.4×10^8 focus-forming units (FFU)/ml. The virus was derived from the Center for Disease Control and Prevention (Atlanta, GA) and amplified at the National Institute of Infectious Diseases (Tokyo, Japan). A viral suspension was kept in small aliquots at −80°C. Each aliquot was thawed in a safety cabinet just before each injection experiment.

Surgical procedures and electrophysiological mapping. For electrophysiological mapping and the subsequent viral injections, a head holder was surgically attached to the monkey's skull under aseptic conditions. The monkeys were sedated with an intramuscular injection of ketamine hydrochloride (5 mg/kg), anesthetized with an intravenous injection of sodium pentobarbital (20 mg/kg), and then positioned in a stereotaxic apparatus. The head holder was fixed on the skull with anchor screws and dental acrylic resin. After recovery periods of several days, the monkeys were anesthetized with an intramuscular injection of ketamine hydrochloride (5–10 mg/kg) and xylazine hydrochloride (0.5–1 mg/kg) and seated in a primate chair with their head fixed in a stereotaxic frame attached to the chair. After partial removal of the skull over the frontal lobe, the precentral gyrus corresponding to the MI was mapped by intracortical microstimulation. A glass-coated elgiloy-alloy microelectrode (0.5–1.5 MΩ at 1 kHz) attached to a manipulator was inserted perpendicular to the dural surface. When trains of 12 cathodal pulses (200 μs duration at 333 Hz; currents of <50 μA) were delivered through a constant-current stimulator, evoked movements of different body parts were carefully examined. To preserve the exposed dural surface, a rectangular chamber was fixed on the skull with acrylic resin.

Viral injection. A few days after the MI mapping, the monkeys received viral injections into the forelimb or hindlimb region of the MI. Under

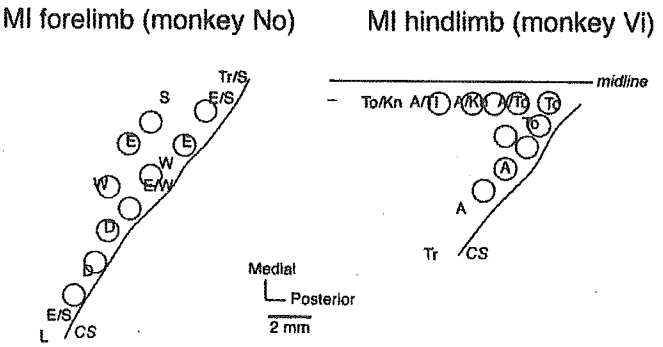

Figure 2. Results of intracortical microstimulation (ICMS) mapping and the sites of rabies virus injection in forelimb (monkey No) or hindlimb (monkey Vi) representation of the MI. Each letter on the cortical surface map denotes the site of electrode penetration, stimulation of which elicited movement predominantly from one of the following body parts: A, Ankle; D, digit (hand); E, elbow; Kn, knee; L, lip; S, shoulder; Tl, tail; To, toe; Tr, trunk; W, wrist; —, locus in which no body movements were elicited by ICMS. Circles indicate the approximate extents of the injection sites. CS, Central sulcus.

Table 1. Summary of experiments

Monkey	Species	Sex	Injection site	Survival (days)	Injection volume (μl)
Ma	J	F	Forelimb	2	8.5
Hu	J	M	Forelimb	3	8
Ke	J	F	Forelimb	3	9
Ir	J	F	Forelimb	3.5	10
Ta	R	M	Forelimb	3.5	9
No	J	M	Forelimb	4	8.5
Ji	R	M	Forelimb	4	10
Qu	R	M	Hindlimb	3	8
Ri	R	M	Hindlimb	4	9
Vi	J	F	Hindlimb	4	10

F, Female; J, Japanese monkey (*Macaca fuscata*); M, male; R, rhesus monkey (*Macaca mulatta*).

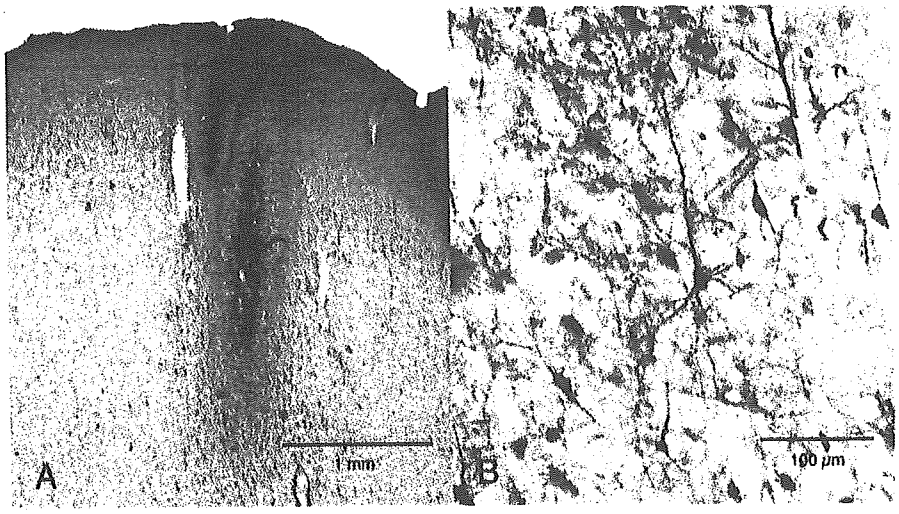

Figure 3. Low- and high-magnification photomicrographs of the injection site in monkey Ma (2 d after the viral injection). In the low-power image (*A*), clusters of labeled neurons are seen around the injection needle track, and in the high-power image (*B*), many neurons are labeled in a Golgi-like manner.

general anesthesia with ketamine hydrochloride (5–10 mg/kg, i.m.) and xylazine hydrochloride (0.5–1 mg/kg, i.m.), each monkey was set in the primate chair in the same manner as in the mapping. A total of 8–10 μl (0.5–1 μl per penetration) of the viral suspension was injected into the identified forelimb or hindlimb region of the MI through a 10 μl Hamilton microsyringe.

Histological procedures. After survival periods of 2–4 d, the monkeys were anesthetized deeply with sodium pentobarbital (50 mg/kg) and perfused transcardially with 0.1 M PBS, pH 7.4, followed by a mixture of 8% formalin and 15% saturated picric acid in 0.1 M phosphate buffer (PB), pH 7.4. The brains were removed from the skull, postfixed in the same fresh fixative overnight, and immersed in PB containing 30% sucrose. Coronal sections were cut serially at 60 μm thickness on a freezing microtome. Every sixth section was immunohistochemically stained for rabies virus with the standard avidin–biotin–peroxidase complex (ABC) method. The detection of rabies virus was performed using a monospecific rabbit antiserum prepared by immunization of His-tagged recombinant nucleoprotein expressed in *Escherichia coli* (Inoue et al., 2003).

The sections were washed briefly in PBS, soaked with 1% skim milk in PBS for 2 h, and then incubated overnight with the primary antibody (diluted at 1:10,000) in PBS containing 0.1% Triton X-100 and 1% normal goat serum. Subsequently, the sections were incubated for 2 h in the same fresh medium containing biotinylated goat anti-rabbit IgG antibody (diluted at 1:200; Vector Laboratories, Burlingame, CA) and reacted with the ABC kit (ABC Elite; Vector Laboratories). For visualization of the antigen, the sections were reacted in 0.05 M Tris-HCl buffer, pH 7.6, containing 0.04% diaminobenzidine, 0.04% nickel chloride, and 0.002% hydrogen peroxide. After washes in PBS, the sections were mounted onto gelatin-coated glass slides. A series of the adjacent sections (60 μm apart) were mounted and Nissl stained with 1% Neutral red or cresyl violet. The areal boundaries in the frontal lobe were determined primarily based on cytoarchitectonic criteria. For the nomenclature of the prefrontal and motor-related areas, the classification of Barbas and Pandya (1987, 1989) was adopted with some modifications (Fig. 1). The caudal and rostral parts of the dorsal premotor cortices (PMdc and PMdr) in the present paper correspond to area 6DC or 6DR, respectively. Whereas the caudal part of the ventral premotor cortex (PMvc) includes area 4C and the caudal part of area 6Va (caudal to the genu of the arcuate sulcus), the rostral part of the ventral premotor cortex (PMvr) includes the rostral part of area 6Va and area 6Vb (rostral to the genu of the arcuate sulcus).

Data analysis. According to electrophysiological mapping data, we prepared the somatotopic map of the MI, which was viewed from the cortical surface. The injection sites of rabies virus in the MI were charted in tracings of equidistant coronal sections and reconstructed on the map. Neuronal labeling in the frontal cortex, the basal ganglia, and the cerebellum was plotted on tracings of representative coronal sections, whereas that in the thalamus was plotted on photomicrographs of corresponding Nissl-stained sections. The number of labeled neurons in each area of the frontal lobe was counted in every 12th section (720 μm apart) by visual inspection under a light microscope. In addition, the distributions of retrograde labeling in the prefrontal cortex in monkeys No and Vi were reconstructed on the unfolded cortical maps. All the unfolded lines were aligned at the fundus of the principal sulcus or, caudally, at the midpoint between the superior and the inferior limb of the arcuate sulcus (Barbas and Pandya, 1987; Hatanaka et al., 2001).

Safety issues. All experiments were performed in a special laboratory (biosafety level 2) designated for *in vivo* virus experiments. Throughout the experiments, the monkeys were kept in individual cages that were placed in the laboratory. To avoid accidental infection with the virus, all investigators received immunization before the present series of experiments and wore protective clothes during the experimental procedures, including viral injection, feeding, and perfusion. Equipment was disinfected with 70% ethanol after each experimental session. Waste was autoclaved before disposal.

Results

Injection sites of rabies virus in forelimb and hindlimb representations of MI

In 10 monkeys, multiple injections of rabies virus were made into forelimb or hindlimb representation of the MI that had been identified electrophysiologically (Fig. 2, Table 1). Seven monkeys received the viral injections into the MI forelimb region and were allowed to survive for 2 d (monkey Ma), 3 d (monkeys Hu and Ke), 3.5 d (monkeys Ir and Ta), or 4 d (monkeys No and Ji). On the other hand, the remaining three monkeys received the viral injections into the MI hindlimb region and were allowed to survive for 3 d (monkey Qu) or 4 d (monkey Ri and Vi). At the 2 d survival period, accumulations of labeled neurons were observed around the needle track of each injection site (Fig. 3*A*). For many labeled neurons, not only their cell bodies but also their dendritic trees were clearly visible (Fig. 3*B*). At the 3–4 d survival periods, dense cell labeling of the injection sites extended for hundreds of micrometers in diameter from the needle tracks. With the different postinjection periods, the distribution patterns of retrograde labeling were analyzed in the frontal lobe, in comparison with those in the basal ganglia and the cerebellum.

On day 2 after viral injection into MI forelimb region

Two days after the viral injection into the forelimb region of the MI, considerable retrograde labeling occurred in the caudal aspects of the nonprimary motor-related areas, which consist of the dorsal and ventral cingulate motor areas (CMAd and CMAv), the supplementary motor area (SMA), and the PMdc and PMvc (see Figs. 1, 4, 7). In contrast, only a small number of labeled neurons were found more rostrally in the frontal lobe (see Fig. 7). At the 2 d postinjection period, many neurons were labeled in the motor thalamus, including the oral division of the ventrolateral nucleus (VLo) and the oral division of the ventroposterolateral nucleus (VPLo) (Fig. 4*I–K*). Some labeled neurons were further observed in other thalamic nuclei, such as the reticular nucleus, the center median

nucleus, and the centrolateral nucleus. More rostrally, labeled neurons were also observed in the basal forebrain (i.e., the substantia innominata; data not shown). However, virtually no neuronal labeling was seen in either the basal ganglia or the cerebellum.

On day 3 after viral injection into MI forelimb region

Three days after the viral injection into the MI forelimb region, many more neurons were labeled in the caudal motor-related areas (see Fig. 7). In addition, areas of dense neuronal labeling in the frontal lobe extended into the rostral aspects of the nonprimary motor-related areas such as the rostral cingulate motor area (CMAr), the presupplementary motor area (pre-SMA), and the PMdr and PMvr (see Figs. 1, 5, 7). On the same day, a number of labeled neurons were also found in prearcuate area 8, corresponding to the frontal eye field (FEF) (Huerta et al., 1987). However, only a few labeled neurons were scattered in the prefrontal cortex. Subcortically, neuronal labeling occurred in both the basal ganglia and the cerebellum (data not shown). The labeled neurons in the basal ganglia were located in the internal segment of the globus pallidus (GPi) ipsilateral to the injection site and, further, in the ventral striatum (Kelly and Strick, 2004). In the cerebellum, the labeled neurons were located in the cerebellar nuclei, especially in the dentate nucleus, contralateral to the injection site.

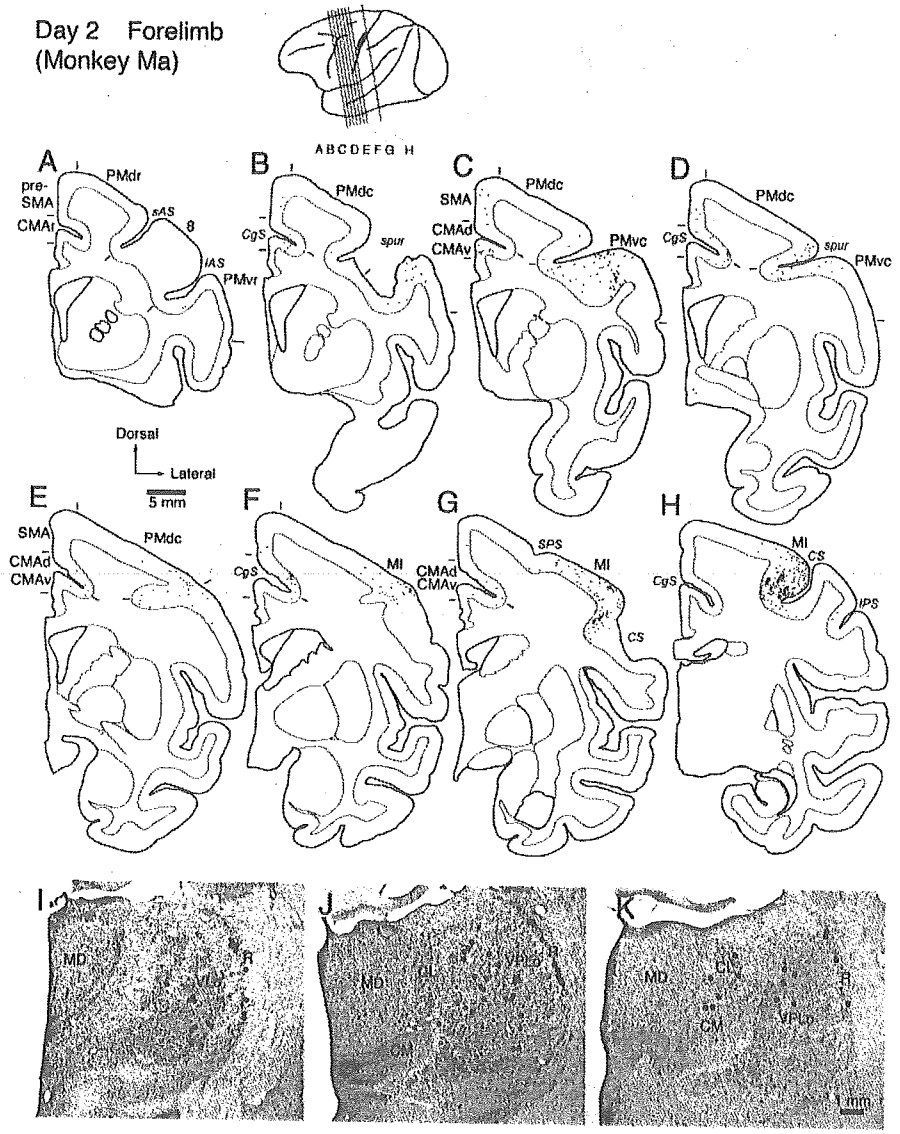

Figure 4. Distribution patterns of retrograde labeling in the frontal lobe (*A–H*) and the thalamus (*I–K*) 2 d after the viral injection into the MI forelimb region (monkey Ma). Eight representative coronal sections through the motor-related areas are arranged rostrocaudally in *A–H*. The approximate rostrocaudal levels of the sections are indicated in the lateral view of the brain. The dark area in this view specifies the extent of the injection site. Photomicrographs of three representative coronal sections through the motor thalamus are arranged rostrocaudally in *I–K*. Each dot in the cortex or the thalamus corresponds to two labeled cells or one labeled cell, respectively. CL, Centrolateral nucleus of the thalamus; CM, center median nucleus of the thalamus; CgS, cingulate sulcus; CS, central sulcus; iAS, inferior limb of the arcuate sulcus; IPS, intraparietal sulcus; MD, mediodorsal nucleus of the thalamus; R, reticular nucleus of the thalamus; sAS, superior limb of the arcuate sulcus; SPS, superior precentral sulcus; spur, spur of the arcuate sulcus; 8, area 8.

On days 3.5 and 4 after viral injection into MI forelimb region

On day 3.5 after the viral injection into the MI forelimb region, the rostral motor-related areas were much more densely labeled (see Fig. 7). Likewise, neuronal labeling in the FEF became more prominent. At the 3.5 d postinjection period, a substantial number of labeled neurons was seen in many areas of the prefrontal cortex. These areas extensively involved areas 24/32 and medial area 9 on the medial wall, lateral area 9 and dorsal area 46 on the dorsolateral surface, ventral area 46 and area 12 on the ventrolateral surface, and areas 11/13 and 14/25 in the ventral aspect (see Fig. 7; for their cytoarchitectonic divisions, see Fig. 1). In each of the prefrontal areas, the number of labeled neurons was greatly increased 4 d after the viral injection (Figs. 6, 7). Among the prefrontal areas, ventral area 46 was most densely labeled, and, also, dense clusters of labeled neurons were distributed in area 12 and the medial wall areas (i.e., areas 24/32 and medial area 9). Our quantitative analysis revealed that the density of labeled neurons in the frontal lobe, especially in the rostral motor-related and prefrontal areas, went up exponentially at a rate of ~100 times per day (Fig. 7*B*).

Moreover, a large number of labeled neurons was located in the basal ganglia and the cerebellum at the postinjection periods of 3.5 and 4 d. Neuronal labeling in the basal ganglia was observed not only in the GPi and the ventral striatum but also in the putamen, the external segment of the globus pallidus, and the subthalamic nucleus (Fig. 6*L*). In the cerebellar nuclei, the labeled neurons were found predominantly in the dentate nucleus and, to a lesser extent, in the interpositus nuclei (Fig. 6*M*). Especially at the 4 d postinjection period, Purkinje cells in the cerebellar cortex were labeled to some extent (Fig. 6*M*).

Differential distributions of neuronal labeling from forelimb versus hindlimb regions of MI

When the virus was injected into the hindlimb region of the MI, many neurons were retrogradely labeled in the frontal motor-related areas with survivals of 3 and 4 d. At the 3 d postinjection

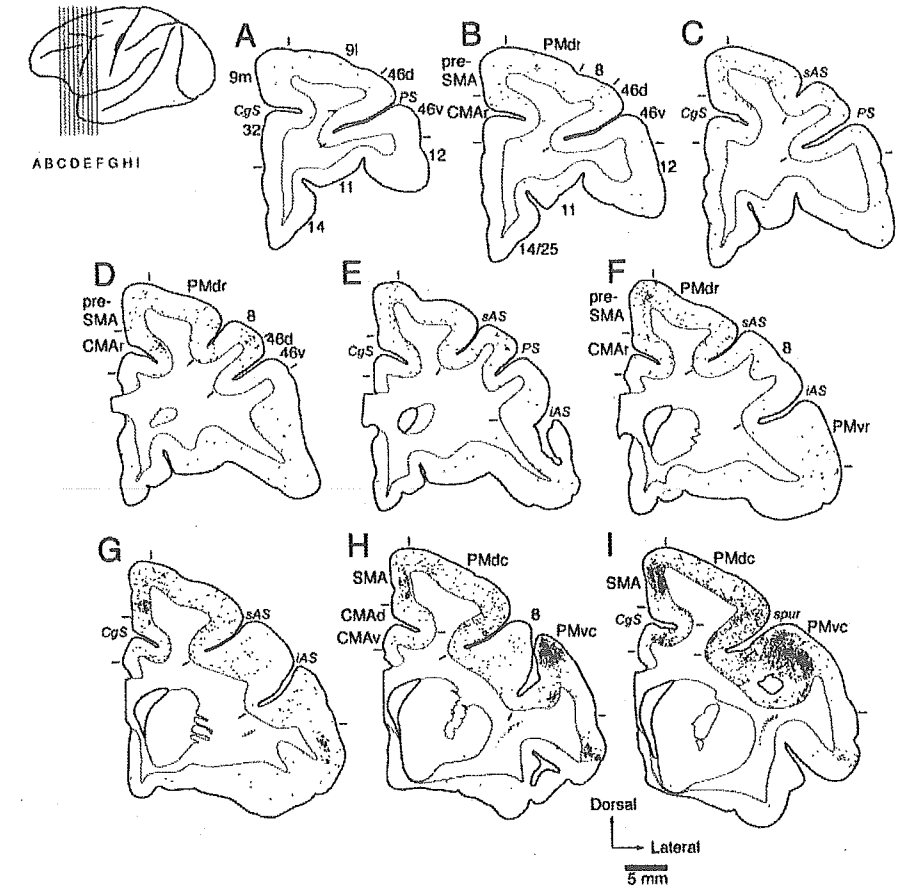

Figure 5. Distribution patterns of retrograde labeling in the frontal lobe 3 d after the viral injection into the MI forelimb region (monkey Hu). Nine representative coronal sections through the motor-related areas and the prefrontal cortex (*A–I*) are arranged rostrocaudally. The approximate rostrocaudal levels of the sections are indicated in the lateral view of the brain. The dark area in this view specifies the extent of the injection site. Each dot corresponds to two labeled cells. CgS, Cingulate sulcus; iAS, inferior limb of the arcuate sulcus; PS, principal sulcus; sAS, superior limb of the arcuate sulcus; spur, spur of the arcuate sulcus; 9l, lateral area 9; 9m, medial area 9; 46d, dorsal area 46; 46v, ventral area 46. Numbers correspond to the area numbers defined by Barbas and Pandya (1989).

period, neuronal labeling was seen abundantly in the caudal motor-related areas. The labeled neurons were distributed mainly in the CMAd and CMAv around the cingulate sulcus and the PMdc medial to the superior precentral sulcus (data not shown). At the 4 d postinjection period, the rostral motor-related areas contained a large number of labeled neurons, especially in the CMAr and PMdr (Fig. 8*C–F*). Neuronal labeling in the prefrontal cortex was also clearly observed (Fig. 8*A*,*B*). The total number of prefrontal neurons labeled from the MI hindlimb region (mean for two monkeys, 3648 cells counted in every 12th section) was 10 times smaller than that in the forelimb-injection case (mean, 38000 cells), although the injected sites in each region covered almost comparable cortical areas (Figs. 2, 9). In addition, the distribution pattern of the labeled neurons from the hindlimb region was different from the distribution pattern of those from the forelimb region (Figs. 9, 10). After the viral injection into the MI hindlimb region, many labeled neurons were located in area 12 and the medial wall areas (i.e., areas 24/32 and medial area 9). Other prefrontal areas exhibited sparse neuron labeling. Of particular interest was that only a few labeled neurons were found in ventral area 46 that was most densely labeled from the MI forelimb region (Figs. 9, 10). Similar findings were obtained in the FEF (i.e., prearcuate area 8). Although strong labeling of FEF neurons was seen 4 d after the viral injection into the MI forelimb region, the FEF was essentially devoid of labeled neurons (Figs. 8, 9).

On days 3 and 4 after the viral injection into the MI hindlimb region, neuronal labeling was evident in the basal ganglia on the same side and in the cerebellum on the opposite side. Especially at the postinjection period of 4 d, dense clusters of labeled neurons in the pallidal complex and the putamen were observed more dorsally than those seen after the injection into the MI forelimb region (compare Figs. 6*L*, 8*I*). The distribution pattern in the putamen of neuronal labeling from the forelimb and hindlimb regions was in good accordance with the topography of corticostriatal terminals from these MI regions (Flaherty and Graybiel, 1993; Takada et al., 1998; Kelly and Strick, 2004). The labeled neurons in the cerebellar nuclei (i.e., the dentate and interpositus nuclei) were distributed predominantly in their rostral portions, whereas those in the forelimb-injection case were distributed more caudally (compare Figs. 6*M*, 8*K*). At the 4 d postinjection period, a number of Purkinje cells were labeled more rostrally in the cerebellar cortex than those in the forelimb-injection case (compare Figs. 6*M*, 8*J*). Thus, our findings revealed that the somatotopic arrangement (forelimb vs hindlimb) of the basal ganglia and the cerebellum was in favor of the previously reported patterns (Hoover and Strick, 1999; Dum and Strick, 2003; Kelly and Strick, 2003, 2004).

Discussion

To use rabies virus for visualization of multisynaptic connections, it is crucial to determine the specificity and rate of transneuronal labeling. For this purpose, we first examined the time-dependent spread of subcortical labeling after viral injections into the MI forelimb region. Consistent with the results of the studies of Kelly and Strick (2003, 2004), neuronal labeling occurred sequentially along the known cortico-basal ganglia and cortico-cerebellar pathways. Two days after the injection, thalamic neurons were labeled mainly in the VLo and VPLo that project to the MI directly. Relatively sparse labeling of these thalamic neurons indicates that a little longer time than 2 d may be needed for sufficient labeling of first-order neurons (for comparison with conventional tracing, see Holsapple et al., 1991; Shindo et al., 1995). At a 3 d postinjection period, both the GPi and the cerebellar nuclei contained labeled neurons. On the fourth day, neuronal labeling in the putamen and the cerebellar cortex became prominent. These results suggest that it takes ~2 d for first-order neuron labeling and 1 additional day per synapse for the subsequent transneuronal labeling. It should be noted, however, that the time course of transneuronal labeling seems somewhat different among neuron types, as shown in the rat brainstem (Ugolini, 1995). For example, reticular thalamic neurons that have no direct projection to the MI were labeled at a 2 d survival. This may

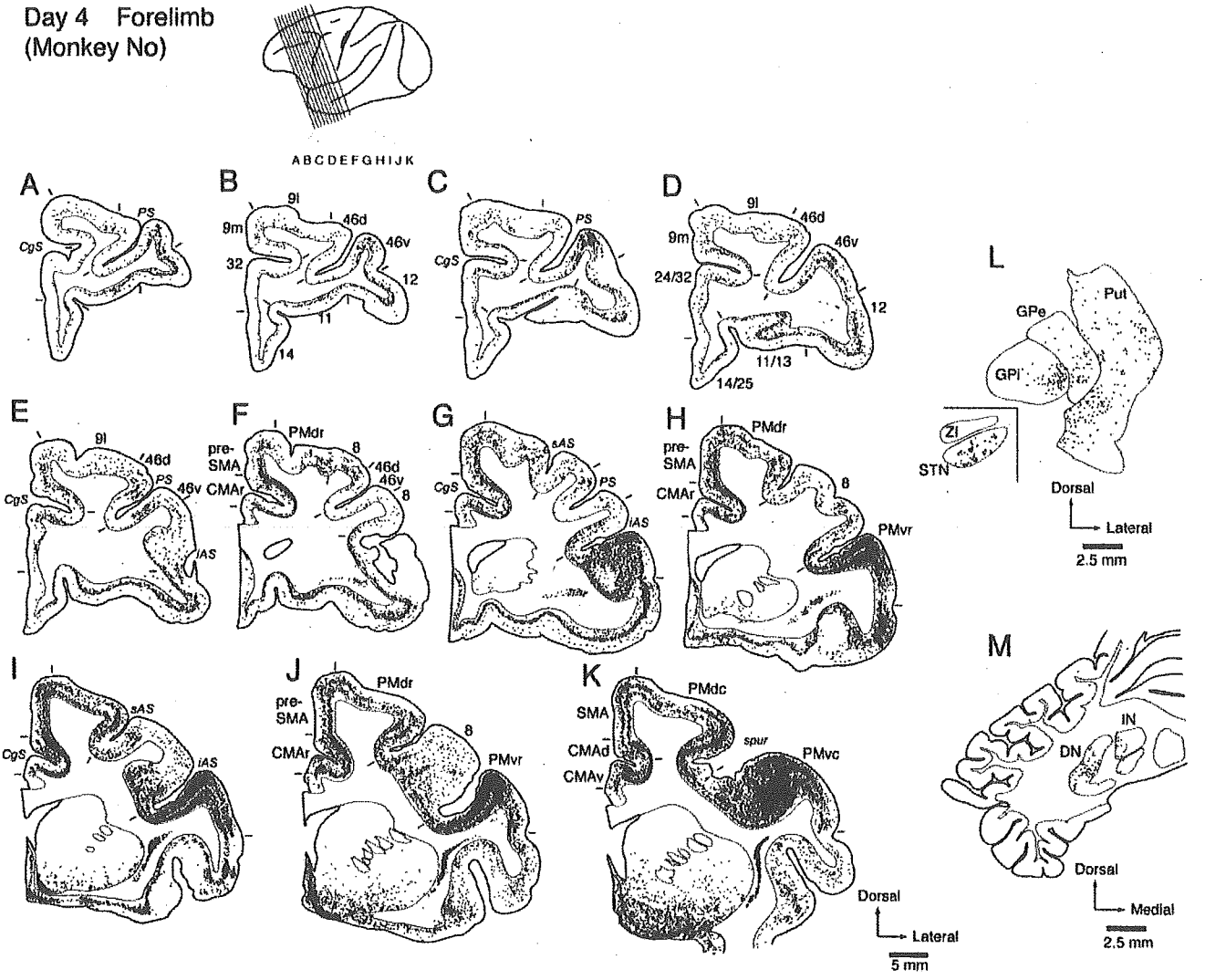

Figure 6. *A–K*, Distribution patterns of retrograde labeling in the frontal lobe 4 d after the viral injection into the MI forelimb region (monkey No). Eleven representative coronal sections through the prefrontal cortex are arranged rostrocaudally (sections *G–J* represent the levels of the rostral motor-related areas). The approximate rostrocaudal levels of the sections are indicated in the lateral view of the brain. The dark area in this view specifies the extent of the injection site. *L*, *M*, Distribution patterns of retrograde labeling in the basal ganglia (*L*) and the cerebellum (*M*). In *L*, clusters of labeled neurons in the internal and external segments of the globus pallidus (GPe) and the putamen (Put) are distributed mainly in their ventral or ventrolateral portions. Note that another cluster of labeled neurons is located far ventromedially within the putamen (Kelly and Strick, 2004). In *A–M*, each dot corresponds to two labeled cells. CgS, Cingulate sulcus; DN, cerebellar dentate nucleus; iAS, inferior limb of the arcuate sulcus; IN, cerebellar interpositus nucleus; PS, principal sulcus; sAS, superior limb of the arcuate sulcus; spur, spur of the arcuate sulcus; STN, subthalamic nucleus; ZI, zona incerta; 9l, lateral area 9; 9m, medial area 9; 46d, dorsal area 46; 46v, ventral area 46. Numbers correspond to the area numbers defined by Barbas and Pandya (1989).

be attributable to exceptionally fast labeling of second-order neurons through the VLo and VPLo, because it has been reported that those neurons are readily labeled in a transsynaptic manner (Itoh et al., 1984). Furthermore, striatal projection neurons tended to be more readily labeled as third-order neurons than cerebellar Purkinje cells. On the other hand, neuronal labeling in the ventral striatum may possibly be attributed to second-order labeling via cholinergic neurons in the basal forebrain that project to the MI monosynaptically, because the basal forebrain labeled initially at a 2 d survival receives input from the ventral striatum, in which labeled neurons were found at a 3 d survival (Haber et al., 1990).

In the frontal cortex, retrograde labeling at a 2 d postinjection period occurred in the caudal motor-related areas, the PMdc, PMvc, SMA, CMAd, and CMAv, that send projection fibers directly to the MI (Muakkassa and Strick, 1979; Tokuno and Tanji, 1993; Hatanaka et al., 2001). At this stage, neurons in the rostral motor-related areas were only sparsely labeled, although part of the areas (i.e., the CMAr) has relatively weak projections to the MI (Dum and Strick, 1991; Takada et al., 2004). On the third day, substantial neuronal labeling extended over the rostral motor-related areas, including the PMdr, PMvr, pre-SMA, and CMAr. Because these areas were labeled simultaneously with the GPi and the cerebellar nuclei, the labeled neurons may probably correspond to second-order neurons. Likewise, many of the labeled neurons in the prefrontal cortex can be considered third-order neurons, because conspicuous labeling of striatal neurons and Purkinje cells appeared coincidently. Our quantitative analysis has revealed that the number of labeled neurons was increased exponentially, first in the caudal motor-related areas, then in the rostral motor-related areas, and finally in the prefrontal areas (Bates and Goldman-Rakic, 1993; Luppino et al., 2003; Takada et al., 2004). In addition, the rapid increase in labeled neuron number could be ascribed to transneuronal labeling through intrinsic and/or bypath circuits. It should also be emphasized here that viral transport might not necessarily be restricted to the frontal

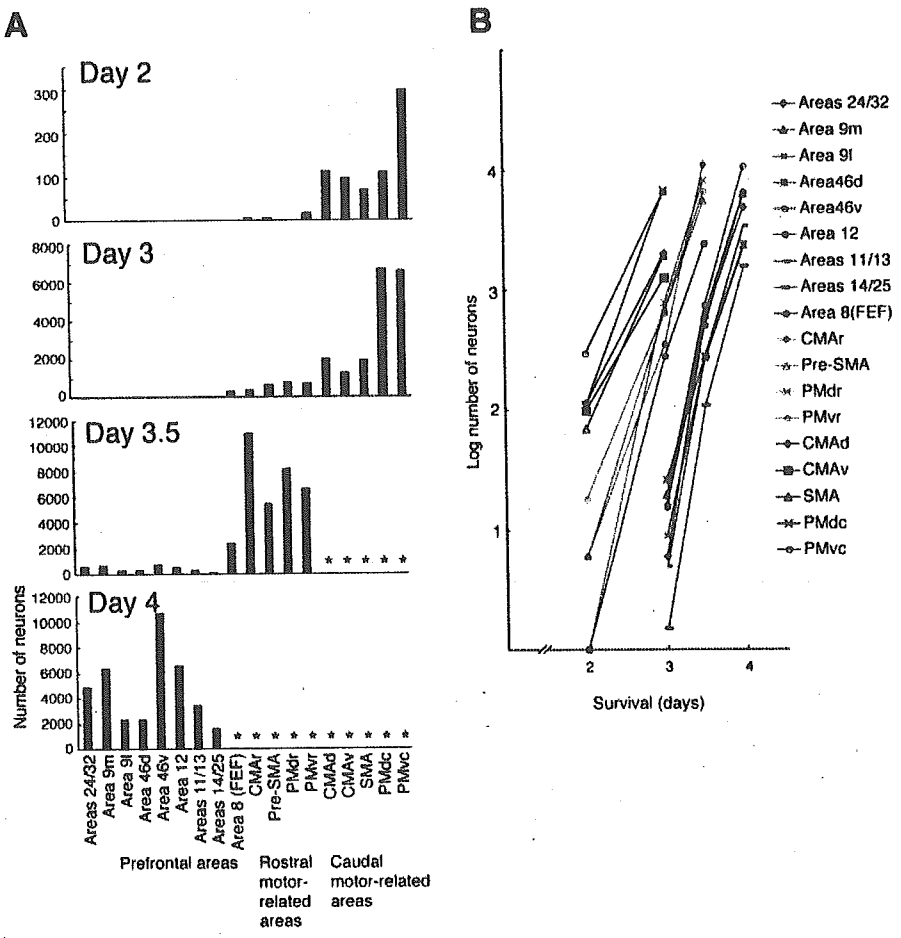

Figure 7. *A*, Diagrams showing the time-dependent changes in the number of labeled neurons in the frontal lobe. Cell counts were performed in every 12th section (60 μm thick; 720 μm apart). The cell number obtained at the 3, 3.5, or 4 d postinjection period is the average of data in monkeys Hu and Ke, Ir and Ta, or No and Ji, respectively, whereas the cell number at the 2 d postinjection period is taken from monkey Ma (see Table 1). Asterisks indicate the areas in which cell counts were not performed, because a tremendous number of neurons were labeled at the 3.5 and 4 d postinjection periods. *B*, Exponential increases in labeled neuron number with the postinjection period. The ordinate indicates the logarithm for the number of labeled neurons in each area. Black symbols represent the caudal motor-related areas, blue symbols represent the rostral motor-related areas, and red symbols represent the prefrontal areas. Filled purple circles represent area 8 (FEF). 9l, Lateral area 9; 9m, medial area 9; 46d, dorsal area 46; 46v, ventral area 46. Numbers correspond to the area numbers defined by Barbas and Pandya (1989).

lobe. The posterior parietal cortex, for instance, may mediate transport from the MI to the premotor and prefrontal areas (Cavada and Goldman-Rakic, 1989; Stanton et al., 1995). Labeling of prefrontal areas may be achieved via the ventral striatum–basal forebrain–MI link (Haber et al., 1990; Ferry et al., 2000).

The primary goals of the present study were (1) to elucidate whether or not the forelimb might specifically be represented in particular areas of the prefrontal cortex and (2) to explore whether or not the forelimb versus the hindlimb might differentially be represented in the prefrontal cortex.

The present results have demonstrated that ventral area 46 was most strongly labeled with rabies virus injected into forelimb representation of the MI. In contrast, dorsal area 46 exhibited much weaker labeling. This indicates that ventral area 46, but not dorsal area 46, is preferentially involved in the control of forelimb movements, albeit both areas are directly interconnected with the rostral motor-related areas (Arikuni et al., 1980; Barbas and Pandya, 1987; Lu et al., 1994; Takada et al., 2004). Consistent with our findings, previous physiological studies have reported that ventral area 46 neurons were specifically activated during the performance of delayed response tasks, in which monkeys responded manually (di Pellegrino and Wise, 1991; Hoshi et al., 1998; Rainer et al., 1998). On the other hand, both ventral and dorsal area 46 neurons responded to delayed oculomotor tasks (Funahashi et al., 1990, 1991). From an anatomical point of view, ventral area 46 and area 12 receive inputs mainly from the posterior parietal cortex (primarily area 7b) and the inferior temporal cortex, respectively (Barbas and Mesulam, 1985; Barbas, 1988; Cavada and Goldman-Rakic, 1989; Seltzer and Pandya, 1989; Carmichael and Price, 1995b). Moreover, it has been shown that posterior parietal neurons respond to forelimb movements as well as to somatosensory or visual stimuli (Dong et al., 1994; Calton et al., 2002).

The medial prefrontal cortex, including areas 24/32 and medial area 9, was another site of dense labeling from the MI forelimb region. Anatomical data to date indicate that these areas have direct interconnections with the rostral motor-related areas, such as the pre-SMA, CMAr, and PMdr (Barbas and Pandya, 1987; Luppino et al., 1993). Also, the medial prefrontal areas receive limbic (emotional or motivational) information from the amygdala and the parahippocampal cortex, as well as polymodal sensory information from the superior temporal cortex and the granular insular cortex (Barbas, 1988; Seltzer and Pandya, 1989; Barbas et al., 1999). Recently, physiological studies in humans and nonhuman primates have suggested that the medial prefrontal areas, including regions in the anterior cingulate cortex, participate in the selection of motor behaviors based on context or reward (Paus, 2001; Swick and Turken, 2002; Dreher and Grafman, 2003; Isomura et al., 2003; Matsumoto et al., 2003). Thus, the strong connectivity to the MI forelimb region implies that the medial prefrontal areas may be responsible for cognitive control of forelimb movements.

To address the issue on prefrontal representations of the forelimb versus the hindlimb, we compared the distribution patterns of prefrontal labeling from both regions of the MI. In the prefrontal cortex, much fewer neurons were labeled from the hindlimb than forelimb region. Ventral area 46, which had the densest labeling from forelimb representation, displayed only sparse labeling from hindlimb representation. Instead, the strongest labeling from hindlimb representation was located on the medial wall, especially in areas 24/32 and medial area 9. These findings imply that the medial prefrontal areas might closely be associated with the control of not only forelimb but also hindlimb movements.

In the present study, the viral injection into the MI forelimb region yielded labeling in prearcuate area 8, corresponding to the FEF. Substantial labeling of FEF neurons occurred as early as 3 d after the injection. This timing of transneuronal labeling coincides well with the timing for the rostral motor-related areas rather than the timing for the prefrontal areas. In the hindlimb-injection case, on the other hand, only a few neurons were labeled

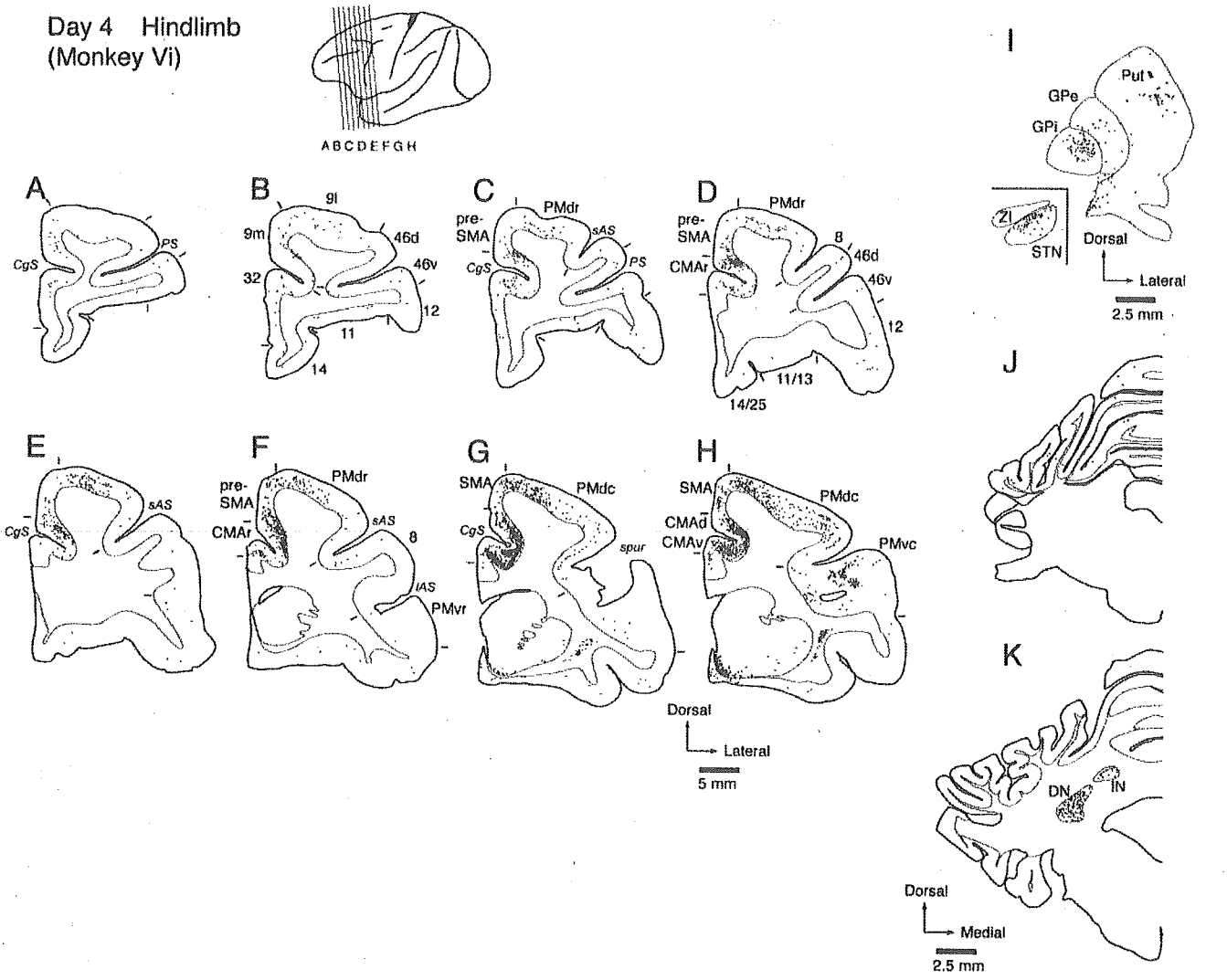

Figure 8. Distribution patterns of retrograde labeling in the frontal lobe (*A–H*), the basal ganglia (*I*), and the cerebellum (*J*, *K*) 4 d after the viral injection into the MI hindlimb region (monkey Vi). Eight representative coronal sections through the prefrontal cortex are arranged rostrocaudally in *A–H*. The approximate rostrocaudal levels of the sections are indicated in the lateral view of the brain. The dark area in this view specifies the extent of the injection site. In *I*, clusters of labeled neurons in the GPi, external segments of the globus pallidus (GPe), and the putamen (Put) are distributed more dorsally than those seen after the viral injection into the MI forelimb region (see Fig. 6*L*). As in the forelimb-injection case, another cluster of labeled neurons is located far ventromedially within the putamen (Kelly and Strick, 2004). In this case, the labeling of Purkinje cells occurs at the rostral level of the cerebellar cortex (*J*), and the labeled neurons in the cerebellar dentate nucleus (DN) and cerebellar interpositus nucleus (IN) are distributed more rostrally than in the forelimb-injection case (see Fig. 6*M*). Each dot in *A–K* corresponds to two labeled cells. CgS, Cingulate sulcus; iAS, inferior limb of the arcuate sulcus; PS, principal sulcus; sAS, superior limb of the arcuate sulcus; spur, spur of the arcuate sulcus; STN, subthalamic nucleus; ZI, zona incerta; 9l, lateral area 9; 9m, medial area 9; 46d, dorsal area 46; 46v, ventral area 46. Numbers correspond to the area numbers defined by Barbas and Pandya (1989).

in the FEF even on the fourth day. These data indicate that the FEF is strongly and specifically interconnected, via one synapse, with the MI forelimb region. This seems intriguing given that the FEF has rarely been implicated in the control of forelimb movements. Two pieces of evidence have addressed the issue on the possible involvement of the FEF in somatic motor control. Arikuni et al. (1988) have reported the existence of reciprocal connections between the FEF and the premotor cortex. Oishi and Kubota (1990) have shown that disinhibition of the FEF with the GABA antagonist bicuculline induces forelimb movements in behaving monkeys. Together, the present results suggest that the FEF is likely to play an essential role not only in the control of eye movements per se, but also in the control of eye–hand coordinative behaviors.

The present data define anatomical evidence for the differential patterns of distribution of prefrontal neurons that are multisynaptically connected with forelimb versus hindlimb representations of the MI. Our results favor a notion that cognitive behaviors based on prefrontal signals must be accompanied more frequently by actions manipulated with the forelimb than those with the hindlimb. Thus, the input systems from the prefrontal cortex to the MI might be developed in a use-dependent manner. Furthermore, the present results indicate that the medial prefrontal areas strongly innervate both the forelimb and the hindlimb regions of the MI in a multisynaptic manner. This suggests that movements of not only the forelimb but also the hindlimb could be influenced by signals derived from the prefrontal areas that receive limbic (amygdalar and hippocampal) inputs.

References

Arikuni T, Sakai M, Hamada I, Kubota K (1980) Topographical projections from the prefrontal cortex to the post-arcuate area in the rhesus monkey, studied by retrograde axonal transport of horseradish peroxidase. Neurosci Lett 19:155–160.

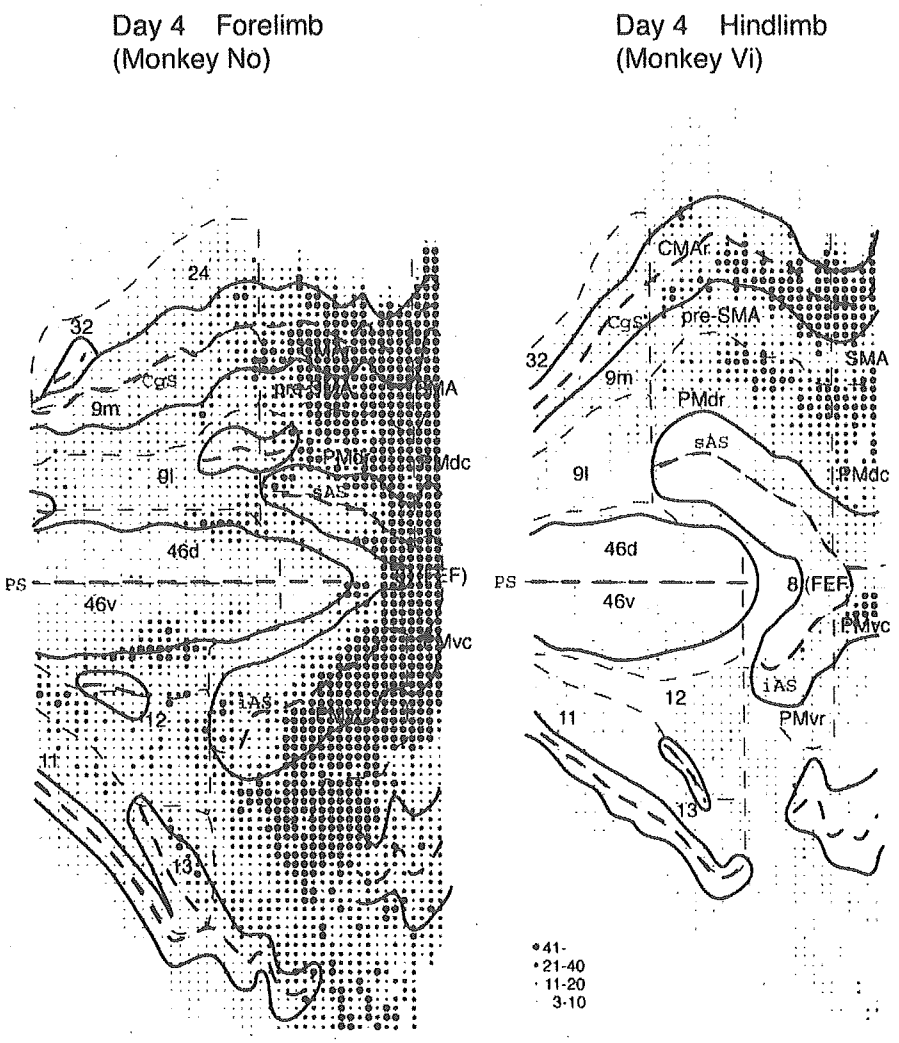

Figure 9. Surface-view reconstructions showing the distribution patterns of labeled neurons in the prefrontal cortex 4 d after the viral injections into the forelimb (monkey No) or hindlimb (monkey Vi) region of the MI. Black solid and dashed lines indicate the gyri and the fundi of the sulci, respectively. Thinner dashed lines denote the boundaries among the prefrontal areas. Four different sizes of filled circles represent the ranges of labeled neuron number. CgS, Cingulate sulcus; iAS, inferior limb of the arcuate sulcus; PS, principal sulcus; sAS, superior limb of the arcuate sulcus; 9l, lateral area 9; 9m, medial area 9; 46d, dorsal area 46; 46v, ventral area 46. Numbers correspond to the area numbers defined by Barbas and Pandya (1989).

Arikuni T, Watanabe K, Kubota K (1988) Connections of area 8 with area 6 in the brain of the macaque monkey. J Comp Neurol 277:21–40.

Barbas H (1988) Anatomic organization of basoventral and mediodorsal visual recipient prefrontal regions in the rhesus monkey. J Comp Neurol 276:313–342.

Barbas H, Mesulam MM (1985) Cortical afferent input to the principalis region of the rhesus monkey. Neuroscience 15:619–637.

Barbas H, Pandya DN (1987) Architecture and frontal cortical connections of the premotor cortex (area 6) in the rhesus monkey. J Comp Neurol 256:211–228.

Barbas H, Pandya DN (1989) Architecture and intrinsic connections of the prefrontal cortex in the rhesus monkey. J Comp Neurol 286:353–375.

Barbas H, Ghashghaei H, Dombrowski SM, Rempel-Clower NL (1999) Medial prefrontal cortices are unified by common connections with superior temporal cortices and distinguished by input from memory-related areas in the rhesus monkey. J Comp Neurol 410:343–367.

Bates JF, Goldman-Rakic PS (1993) Prefrontal connections of medial motor areas in the rhesus monkey. J Comp Neurol 336:211–228.

Calton JL, Dickinson AR, Snyder LH (2002) Non-spatial, motor-specific activation in posterior parietal cortex. Nat Neurosci 5:580–588.

Carmichael ST, Price JL (1995a) Limbic connections of the orbital and medial prefrontal cortex in macaque monkeys. J Comp Neurol 363:615–641.

Carmichael ST, Price JL (1995b) Sensory and premotor connections of the orbital and medial prefrontal cortex of macaque monkeys. J Comp Neurol 363:642–664.

Cavada C, Goldman-Rakic PS (1989) Posterior parietal cortex in rhesus monkey: II. Evidence for segregated corticocortical networks linking sensory and limbic areas with the frontal lobe. J Comp Neurol 287:422–445.

di Pellegrino G, Wise SP (1991) A neurophysiological comparison of three distinct regions of the primate frontal lobe. Brain 114:951–978.

Dong WK, Chudler EH, Sugiyama K, Roberts VJ, Hayashi T (1994) Somatosensory, multisensory, and task-related neurons in cortical area 7b (PF) of unanesthetized monkeys. J Neurophysiol 72:542–564.

Dreher JC, Grafman J (2003) Dissociating the roles of the rostral anterior cingulate and the lateral prefrontal cortices in performing two tasks simultaneously or successively. Cereb Cortex 13:329–339.

Dum RP, Strick PL (1991) The origin of corticospinal projections from the premotor areas in the frontal lobe. J Neurosci 11:667–689.

Dum RP, Strick PL (1996) Spinal cord terminations of the medial wall motor areas in macaque monkeys. J Neurosci 16:6513–6525.

Dum RP, Strick PL (2003) An unfolded map of the cerebellar dentate nucleus and its projections to the cerebral cortex. J Neurophysiol 89:634–639.

Ferry AT, Ongur D, An X, Price JL (2000) Prefrontal cortical projections to the striatum in macaque monkeys: evidence for an organization related to prefrontal networks. J Comp Neurol 425:447–470.

Flaherty AW, Graybiel AM (1993) Two input systems for body representations in the primate striatal matrix: experimental evidence in the squirrel monkey. J Neurosci 13:1120–1137.

Funahashi S, Bruce CJ, Goldman-Rakic PS (1990) Visuospatial coding in primate prefrontal neurons revealed by oculomotor paradigms. J Neurophysiol 63:814–831.

Funahashi S, Bruce CJ, Goldman-Rakic PS (1991) Neuronal activity related to saccadic eye movements in the monkey's dorsolateral prefrontal cortex. J Neurophysiol 65:1464–1483.

Galea MP, Darian-Smith I (1994) Multiple corticospinal neuron populations in the macaque monkey are specified by their unique cortical origins, spinal terminations, and connections. Cereb Cortex 4:166–194.

Georgopoulos AP, Kalaska JF, Caminiti R, Massey JT (1982) On the relations between the direction of two-dimensional arm movements and cell discharge in primate motor cortex. J Neurosci 2:1527–1537.

Haber SN, Lynd E, Klein C, Groenewegen HJ (1990) Topographic organization of the ventral striatal efferent projections in the rhesus monkey: an anterograde tracing study. J Comp Neurol 293:282–298.

Hatanaka N, Nambu A, Yamashita A, Takada M, Tokuno H (2001) Somatotopic arrangement and corticocortical inputs of the hindlimb region of the primary motor cortex in the macaque monkey. Neurosci Res 40:9–22.

He SQ, Dum RP, Strick PL (1993) Topographic organization of corticospinal projections from the frontal lobe: motor areas on the lateral surface of the hemisphere. J Neurosci 13:952–980.

Hikosaka K, Watanabe M (2000) Delay activity of orbital and lateral prefrontal neurons of the monkey varying with different rewards. Cereb Cortex 10:263–271.

Holsapple JW, Preston JB, Strick PL (1991) The origin of thalamic inputs to the "hand" representation in the primary motor cortex. J Neurosci 11:2644–2654.

Hoover JE, Strick PL (1999) The organization of cerebellar and basal ganglia outputs to primary motor cortex as revealed by retrograde transneuronal transport of herpes simplex virus type 1. J Neurosci 19:1446–1463.

Hoshi E, Shima K, Tanji J (1998) Task-dependent selectivity of movement-

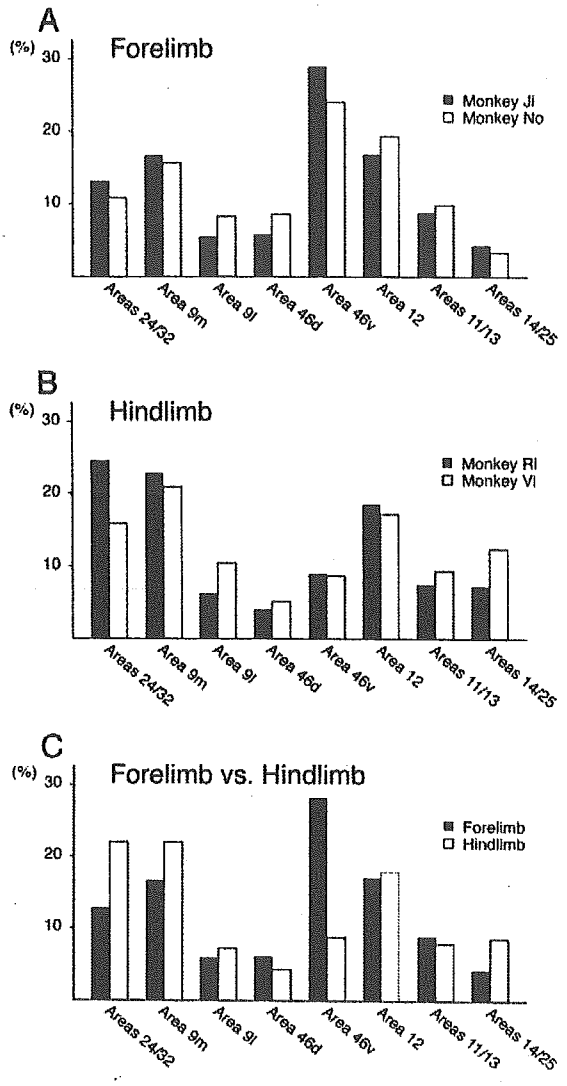

Figure 10. Diagram showing the differential distributions of neuronal labeling in the prefrontal cortex 4 d after the viral injections into the forelimb or hindlimb region of the MI (see also Fig. 9). *A*, *B*, Comparison of data obtained in two monkeys that received the injections into the forelimb region (*A*; monkeys Ji and No) or hindlimb region (*B*; monkeys Ri and Vi). Each bar represents the ratio of the labeled neuron number to the total number of labeled prefrontal neurons. Note that in each of the forelimb- and hindlimb-injection cases, the data are mostly consistent in the two monkeys. *C*, Comparison of the forelimb- versus hindlimb-injection cases. Filled and open bars indicate the average of the data obtained in the two monkeys shown in *A* and *B*, respectively.

related neuronal activity in the primate prefrontal cortex. J Neurophysiol 80:3392–3397.

Huerta MF, Krubitzer LA, Kaas JH (1987) Frontal eye field as defined by intracortical microstimulation in squirrel monkeys, owl monkeys, and macaque monkeys. II. Cortical connections. J Comp Neurol 265:332–361.

Inoue S, Sato Y, Hasegawa H, Noguchi A, Yamada A, Kurata T, Iwasaki T (2003) Cross-reactive antigenicity of nucleoproteins of lyssaviruses recognized by a monospecific anti-rabies virus nucleoprotein antiserum on paraffin sections of formalin-fixed tissues. Pathol Int 53:525–533.

Isomura Y, Ito Y, Akazawa T, Nambu A, Takada M (2003) Neural coding of "attention for action" and "response selection" in primate anterior cingulate cortex. J Neurosci 23:8002–8012.

Itoh K, Yasui Y, Takada M, Mitani A, Kaneko T, Sugimoto T, Mizuno N (1984) An anterograde-retrograde transneuronal transport of conjugates of wheat germ agglutinin with horseradish peroxidase (WGA-HRP): labeling of neurons in the reticular nucleus of the thalamus with WGA-HRP injected into the posterior column nuclei in the cat. Brain Res 323:185–187.

Kakei S, Hoffman DS, Strick PL (1999) Muscle and movement representations in the primary motor cortex. Science 285:2136–2139.

Kelly RM, Strick PL (2000) Rabies as a transneuronal tracer of circuits in the central nervous system. J Neurosci Methods 103:63–71.

Kelly RM, Strick PL (2003) Cerebellar loops with motor cortex and prefrontal cortex of a nonhuman primate. J Neurosci 23:8432–8444.

Kelly RM, Strick PL (2004) Macro-architecture of basal ganglia loops with the cerebral cortex: use of rabies virus to reveal multisynaptic circuits. Prog Brain Res 143:449–459.

Lu MT, Preston JB, Strick PL (1994) Interconnections between the prefrontal cortex and the premotor areas in the frontal lobe. J Comp Neurol 341:375–392.

Luppino G, Matelli M, Camarda R, Rizzolatti G (1993) Corticocortical connections of area F3 (SMA-proper) and area F6 (pre-SMA) in the macaque monkey. J Comp Neurol 338:114–140.

Luppino G, Rozzi S, Calzavara R, Matelli M (2003) Prefrontal and agranular cingulate projections to the dorsal premotor areas F2 and F7 in the macaque monkey. Eur J Neurosci 17:559–578.

Matsumoto K, Suzuki W, Tanaka K (2003) Neuronal correlates of goal-based motor selection in the prefrontal cortex. Science 301:229–232.

Muakkassa KF, Strick PL (1979) Frontal lobe inputs to primate motor cortex: evidence for four somatotopically organized "premotor" areas. Brain Res 177:176–182.

Oishi T, Kubota K (1990) Disinhibition in the monkey prefrontal cortex, by injecting bicuculline, induces forelimb movements learned in a GO/NO-GO task. Neurosci Res 8:202–209.

Pandya DN, Yeterian EH (1990) Prefrontal cortex in relation to other cortical areas in rhesus monkey: architecture and connections. Prog Brain Res 85:63–94.

Paus T (2001) Primate anterior cingulate cortex: where motor control, drive and cognition interface. Nat Rev Neurosci 2:417–424.

Rainer G, Asaad WF, Miller EK (1998) Memory fields of neurons in the primate prefrontal cortex. Proc Natl Acad Sci USA 95:15008–15013.

Sakagami M, Tsutsui K (1999) The hierarchical organization of decision making in the primate prefrontal cortex. Neurosci Res 34:79–89.

Seltzer B, Pandya DN (1989) Frontal lobe connections of the superior temporal sulcus in the rhesus monkey. J Comp Neurol 281:97–113.

Shindo K, Shima K, Tanji J (1995) Spatial distribution of thalamic projections to the supplementary motor area and the primary motor cortex: a retrograde multiple labeling study in the macaque monkey. J Comp Neurol 357:98–116.

Smith JS, Yager PA, Baer GM (1996) A rapid tissue culture test for determining rabies-neutralizing antibody. In: Laboratory techniques in rabies, Ed 4 (Meslin FX, Kaplan MM, Koprowski H, eds), pp 371–373. Geneva: World Health Organization.

Stanton GB, Bruce CJ, Goldberg ME (1995) Topography of projections to posterior cortical areas from the macaque frontal eye fields. J Comp Neurol 353:291–305.

Swick D, Turken AU (2002) Dissociation between conflict detection and error monitoring in the human anterior cingulate cortex. Proc Natl Acad Sci USA 99:16354–16359.

Takada M, Tokuno H, Nambu A, Inase M (1998) Corticostriatal projections from the somatic motor areas of the frontal cortex in the macaque monkey: segregation versus overlap of input zones from the primary motor cortex, the supplementary motor area, and the premotor cortex. Exp Brain Res 120:114–128.

Takada M, Nambu A, Hatanaka N, Tachibana Y, Miyachi S, Taira M, Inase M (2004) Organization of prefrontal outflow toward frontal motor-related areas in macaque monkeys. Eur J Neurosci 19:3328–3342.

Tokuno H, Tanji J (1993) Input organization of distal and proximal forelimb areas in the monkey primary motor cortex: a retrograde double labeling study. J Comp Neurol 333:199–209.

Tremblay L, Schultz W (1999) Relative reward preference in primate orbitofrontal cortex. Nature 398:704–708.

Ugolini G (1995) Specificity of rabies virus as a transneuronal tracer of motor networks: transfer from hypoglossal motoneurons to connected second-order and higher order central nervous system cell groups. J Comp Neurol 356:457–480.

Wilson FA, Scalaidhe SP, Goldman-Rakic PS (1993) Dissociation of object and spatial processing domains in primate prefrontal cortex. Science 260:1955–1958.

Epidemiol. Infect. (2005), **000**, 1–12. © 2005 Cambridge University Press
doi:10.1017/S0950268805004139 Printed in the United Kingdom

Non-polio enterovirus isolation among families in Ulaanbaatar and Tov province, Mongolia: prevalence, intrafamilial spread, and risk factors for infection

M. KURAMITSU[1], C. KUROIWA[1]*, H. YOSHIDA[2], M. MIYOSHI[1], J. OKUMURA[1], H. SHIMIZU[2], L. NARANTUYA[3] AND D. BAT-OCHIR[4]

[1] *Department of Health Policy and Planning, Graduate School of Medicine, the University of Tokyo, Tokyo, Japan*
[2] *Department of Virology II, National Institute of Infectious Diseases, Tokyo, Japan*
[3] *Public Health Institute, Ministry of Health, Ulaanbaatar, Mongolia*
[4] *National Center for Communicable Disease, Ministry of Health, Ulaanbaatar, Mongolia*

(*Accepted 7 February 2005*)

SUMMARY

Studies of non-polio enterovirus prevalence and transmissibility in developing countries are limited and few studies have investigated specific risk factors for infection. An epidemiological survey of non-polio enterovirus among families in Mongolia was conducted in the late summer of 2003. Stools of 122 healthy persons were collected weekly for 5 weeks. Eight serotypes of non-polio enteroviruses (echovirus 30, 33, 12, 25, coxsackievirus A10, A2, A4, A24) were isolated from 62 persons, with an overall isolation rate of 51%, and 64% and 35% among children under 10 years and adults over age 21 years. Fifty-four per cent of isolations were due to intrafamilial infection. Analysis of risk factors for infection suggested contamination of indoor kitchen, bathroom, toilet, and waste disposal area. Hand washing after defecation was protective against infection. Our study findings stress the importance of hand washing and cleaning hygienic facilities to prevent infection by enteric viruses in the home environment.

INTRODUCTION

Though most enterovirus infections are asymptomatic, enterovirus can become a serious public health concern with a capability of causing a spectrum of clinical illnesses such as paralysis, aseptic meningitis, encephalitis, herpangina, hand, foot, and mouth disease, upper respiratory disease, cardiac disease, and acute haemorrhagic conjunctivitis [1–3]. Enterovirus prevalence and transmissibility vary by factors such as climate, geography, crowding, and socio-economic status; previous studies among healthy individuals in different countries have shown diversity in isolation rate [4–13]. However, studies of enterovirus, especially non-polio enterovirus, in developing countries are limited and few studies have investigated specific risk factors for infection.

In Mongolia, enteric diseases are widespread, imposing a heavy burden on the population's health. Hepatitis A is considered highly endemic: 8250 cases were clinically diagnosed as hepatitis A in 2000 among the national population of 2·7 million [14]. Diarrhoea is a significant problem resulting in a high infant mortality rate which was 51·97/1000 births as of 2002 [15]. Despite our knowledge that enteric diseases are endemic, no study has been done on non-polio enterovirus prevalence and transmissibility in Mongolia.

Therefore, this study aims to determine non-polio enterovirus prevalence in urban areas of Mongolia, to attempt isolation of enterovirus from hand, to assess

* Author for correspondence: Dr C. Kuroiwa, The University of Tokyo, Graduate School of Medicine, Department of Health Policy and Planning, 7-3-1, Hongo, Bunkyo-ku, Tokyo 113-0033, Japan. (Email: ckuroiw@m.u-tokyo.ac.jp)

the degree of intrafamilial spread of non-polio enterovirus as a measure of its transmissibility, and to investigate risk factors for non-polio enterovirus infection such as living environment and hygiene practices.

METHODS

Study site

This study was conducted from July to August 2003 in Ulaanbaatar and Tov province in Mongolia. Four districts were chosen from Ulaanbaatar: Chingeltei, Bayangol, Bayanzurkh, and Songinokhairkhan. From Tov province, Zuum mod (provincial centre) and Bayanchandmani (provincial district centre) were selected. Areas with different living environments such as type of residence and water supply were considered for site selection.

Areas within the six districts can be classified into three distinct categories: slum area in Ulaanbaatar, apartment area in Ulaanbaatar, and remote but accessible area from Ulaanbaatar (Zuum mod and Bayanchandmani). In Ulaanbaatar, *gers* (traditional Mongolian dwelling consisting of tent-like wooden structure covered with felt, no inside hygienic facilities) and houses (structure with one or more rooms, some with piped water and/or inside hygienic facilities) co-exist on dirt roads in slum areas, whereas apartment (provided with piped water and hygienic facilities) areas have paved roads and often have local shopping centres. Zuum mod and Bayanchandmani are located 45 and 80 km from Ulaanbaatar and are surrounded by grassland and gentle hills.

Study population and oral poliovirus vaccine (OPV) administration

Four to five infants who were scheduled for OPV immunization during July 2003 and their families were consecutively sampled in each of the six areas. An infant (study child), mother, father, and one youngest sibling were included in the study from each household. For some cases, a relative living in the same household as the study child, or a contact of a sibling of the study child who lived in a different household were sampled for investigation. OPV (SB Biologicals, Rixensart, Belgium) was administered to study children under routine immunization on the first week.

Sample collection

Stool specimens were collected from all participants at weekly intervals for 5 weeks. Swab samples were taken from palms and fingers of 46 available subjects who took care of study children on the second week. Swabs soaked in 1 ml PBS (Nissui, Tokyo, Japan) were used. All samples were carried at 4 °C and stored at −20 °C. Interviews to determine living environment and hygiene practices were conducted using a semi-structured questionnaire. Questions on living environment of each household were asked of the mother or father, and questions on hygiene behaviour were asked of all subjects except study children. For children too young to answer questions, the mothers answered for them. This did not seem inappropriate as in the case of very young children the mothers instructed them in hygienic activities or they did those activities together. The questionnaire was reviewed and revised by health workers participating in the study.

Ethical approval was obtained from the University of Tokyo Ethical Committee, and approval was given by the Ministry of Health in Mongolia. Written informed consent was collected from all participants or their guardians.

Isolation and identification of enterovirus in stools

Virus isolation was done according to the WHO recommended method [16] with the following modifications. Stool extracts were treated with PBS containing 10% chloroform and stored at −20 °C until inoculation onto rhabdomyosarcoma (RD), HEp-2 and L20B cell lines. Isolation was conducted using 24-well plates. Two sequential passages of 7 days were performed in the three cell lines before recording as negative. Samples which showed a cytopathic effect (CPE) in RD and/or HEp-2 cells after 14 days of observation were passaged to L20B cells and observed for another week. For samples which showed CPE in L20B cells, identification for poliovirus was conducted. For samples which showed CPE in RD and/or HEp-2 cells but not in L20B cells, identification for non-polioviruses was performed using enterovirus antisera (RIVM, Bilthoven, The Netherlands). For samples which were poliovirus positive in L20B cells and also showed CPE in RD and/or HEp-2 cells, samples were analysed for concurrent non-polio enterovirus infection. A total of 50 μl of diluted tissue culture fluid from RD and/or HEp-2 cells was mixed with 50 μl of antiserum to poliovirus types 1+2+3 in RD and/or HEp-2 cells respectively, and observed for 1 week. For CPE-positive samples, virus fluid was re-inoculated onto

L20B cells to confirm the absence of poliovirus and observed for another week.

RNA extraction and RT–PCR

For non-poliovirus samples for which a virus serotype could not be identified by neutralization using the RIVM kit, viral RNA was extracted from 140 μl of infected cell culture fluid using QIAamp Viral RNA kit (Qiagen, Hilden, Germany). Extracted RNA (5 μl) was used for genomic amplification by RT–PCR using Access RT–PCR kit (Promega, Madison, WI, USA). RT–PCR was conducted using 50 pmol of primers OL68-1 (5′-GGTAAYTTCCACCACCA-NCC-3′, antisense) and EVP4 (5′-CTACTTTGGG-TGTCCGTGTT-3′, sense) in the 5′NTR-VP4-VP2 region [17]. The condition for RT–PCR was 45 min at 48 °C, 2 min at 94 °C, 35 cycles at 94 °C for 10 s, 50 °C for 10 s, 65 °C for 1 min, and 5 min at 65 °C.

Sequencing analysis

Amplified products were purified using QIAquick PCR purification kit (Qiagen). Nucleotide sequencing reaction was performed using ABI PRISM BigDye Termination Cycle Sequencing kit with 3·2 pmol of each primer (Applied Biosystems, Foster City, CA, USA). Sequence data were collected using ABI PRISM 3100 Avant Genetic Analyzer (Applied Biosystems).

For non-polio enteroviruses, clusters of each virus type were made by Clustal W software after 1000 times bootstrapping [18], using their nucleotide sequences in the 5′NTR-VP4-VP2 region identified using OL68-1 and EVP4 primers. (The same method was used for the analysis of intrafamilial spread of non-polio enteroviruses.) One sample in each virus type was chosen and its virus type was determined by RT–PCR using 187 (5′-ACIGCIGYIGARACIGG-NCA-3′, sense), 188 (5′-ACIGCIGTIGARACIGG-NG-3′, sense), 189 (5′-CARGCIGCIGARACIGG-NGC-3′, sense), 222 (5′-CICCIGGIGGIAYRWA-CAT-3′, antisense), 012 (5′-ATGTAYGTICCICCI-GGIGG-3′, sense), 040 (5′-ATGTAYRTICCIMCI-GGIGC-3′, sense), and 011 (5′-GCICCIGAYTGI-TGICCRAA-3′, antisense) in the VP1 region [19]. A total of 20 pmol of each antisense primer and 40 pmol of sense primer were used for the RT–PCR reaction with the same cycle condition as above.

Previously reported sequences used in the comparison were obtained from GenBank. Molecular-based enterovirus typing method described by Oberste et al. [20] was used with nucleotide sequence data of VP1 region.

Restriction fragment length polymorphism (RFLP) analysis

For samples positive for poliovirus, RFLP analysis was conducted for intra-typic differentiation to distinguish between vaccine and wild polioviruses [21]. The purified PCR products were digested with *Dde*I, *Hpa*II, and *Hae*III (Takara, Kyoto, Japan) at 37 °C for 2 h. The digested fragments were electrophoresed on 2% agarose gel.

Detection of enterovirus on hands

RNA was extracted from 980 μl PBS in which the swab was soaked. RT–PCR was conducted using 19 μl RNA and 80 pmol of EVP4-OL68-1 primers and UG1-UC1 (5′-GAATTCCATGTCAAATCT-AGA-3′, sense) primers [21] with the same condition as with stool samples. Subsequently, nested PCR was conducted using puReTaq Ready-To-Go PCR beads (Amersham Biosciences, Piscataway, NJ, USA) with 1 μl PCR product of EVP4 and OL68-1 and 20 pmol of OL68-1 and OL24 (5′-CTACTTTGGGTGTCCG-3′, sense) primers [22] in a 25 μl reaction. PCR products were electrophoresed in 2% agarose gels.

Statistics

Univariate analysis was conducted to screen statistically significant ($P<0·05$) variables: χ^2 tests for categorical data and Student's t test for continuous data were adopted. Fisher's exact test was applied for data with small frequencies and Yates' correction was used with 2×2 categorical data. Logistic regression was performed for each significant variable and odds ratios were calculated for each risk factor. Analysis of variance (ANOVA) was conducted for analysis of factors associated with degree of intrafamilial spread, and $P<0·1$ was considered significant due to the small number of households analysed. The degree of intrafamilial spread was calculated by dividing the number of family member(s) infected by the total number of family members in the household. In the analysis of association between hygiene practices and non-polio enterovirus isolation, infants were excluded from analysis due to the difficulty in acquiring accurate data on their behaviour. For the analysis of factors associated with the degree of intrafamilial

Table 1. *Enterovirus isolated from stool specimens collected from families in Ulaanbaatar and Tov province, Mongolia, late summer 2003, by age*

		Age group (years)													
		0–1		2–10		11–20		21–30		31–40		41+		Total	
Virus		30 tested		23 tested		12 tested		37 tested		12 tested		8 tested		122 tested	
Group	Type	No.	(%)	No.	(%)	No.	(%)	No.	(%)	No.	(%)	No.	(%)	No.	(%)
Polio	1	9	(30)	1	(4·3)	1	(8·3)	1	(2·7)	0	(0)	0	(0)	12	(9·8)
	2	5	(16·7)	0	(0)	0	(0)	0	(0)	0	(0)	0	(0)	5	(4·1)
	3	6	(20)	0	(0)	0	(0)	0	(0)	1	(8·3)	0	(0)	7	(5·7)
Total persons shedding poliovirus*		15	(50)	1	(4·3)	1	(8·3)	1	(2·7)	1	(8·3)	0	(0)	19	(15·6)
Concurrent infections†		1 P1+P2‡ 3 P1+P3‡ 1 P2+P3													
Echo	30	7	(23·3)	9	(39·1)	0	(0)	5	(13·5)	4	(33·3)	1	(12·5)	26	(21·3)
	33	7	(23·3)	6	(26·1)	6	(50)	9	(24·3)	1	(8·3)	0	(0)	29	(23·8)
	12	1	(3·3)	0	(0)	0	(0)	0	(0)	0	(0)	0	(0)	1	(0·8)
	25	1	(3·3)	1	(4·3)	0	(0)	0	(0)	0	(0)	0	(0)	2	(1·6)
	Total*	16	(53·3)	16	(69·6)	6	(50)	14	(37·8)	5	(41·7)	1	(12·5)	58	(47·5)
Coxsackie	A10	4	(13·3)	3	(13)	1	(8·3)	0	(0)	0	(0)	0	(0)	8	(6·6)
	A2	0	(0)	1	(4·3)	0	(0)	0	(0)	0	(0)	0	(0)	1	(0·8)
	A4	0	(0)	1	(4·3)	0	(0)	0	(0)	0	(0)	0	(0)	1	(0·8)
	A24	0	(0)	0	(0)	1	(8·3)	0	(0)	0	(0)	0	(0)	1	(0·8)
	Total*	4	(13·3)	5	(21·7)	2	(16·7)	0	(0)	0	(0)	0	(0)	11	(9)
Total persons shedding non-polio enterovirus*		17	(56·7)	17	(73·9)	8	(66·7)	14	(37·8)	5	(41·7)	1	(12·5)	62	(50·8)
Concurrent infections†		1 1 E33+CA10		2 E33+CA10 1 E33+CA4‡ 1 E30+CA10											

* There are individuals infected with multiple virus types during the course of 5 weeks; such individuals are counted as one.
† Number of persons concurrently yielding multiple virus types during the course of 5 weeks.
‡ P1, poliovirus type 1; P2, poliovirus type 2; P3, poliovirus type 3; E30, echovirus 30; E33, echovirus 33; CA10, coxsackie A10; CA4, coxsackie A4.

spread, one study child who lived in an orphanage was excluded. Statistic analysis was performed using SPSS 11.0.1J (SPSS Japan Inc., Tokyo, Japan).

RESULTS

Demographic characteristics

A total of 29 households involving 122 subjects participated in the study. The mean age of the study children was 3·9 months [± standard deviation (S.D.) 1·0 month], siblings 5·9 ± 4·1 years, mothers 26·6 ± 5·4 years, fathers 28·9 ± 5·9 years, relatives 30·1 ± 17·1 years, and contacts of siblings 29·7 ± 23·2 years. A total of 70/122 (57%) of subjects were female. From Chingeltei, Bayangol, Songinokhairkhan, Bayanzurkh, Zuum mod, and Bayanchandmani, 25, 17, 23, 20, 23, and 14 subjects respectively, participated.

Poliovirus and non-polio enterovirus isolation

Poliovirus isolation status is shown in Table 1. Fifteen study children (50%) excreted poliovirus, and polioviruses were isolated from four familial contacts: one sibling (age 2 years), two mothers (ages 21 and 34 years), and one uncle (age 16 years). Intra-typic differentiation revealed all polioviruses to be Sabin-like (vaccine type).

Table 2. *Non-polio enterovirus isolated from stool specimens collected from families in Ulaanbaatar and Tov province, Mongolia, late summer 2003, by sex and age*

Age group (years)	Female		Male	
	%	(No. positive /no. tested)	%	(No. positive /no. tested)
0–1	43	(6/14)	69	(11/16)
2–10	64	(7/11)	83	(10/12)
11–20	70	(7/10)	50	(1/2)
21–30	39	(9/23)	36	(5/14)
31–40	50	(3/6)	33	(2/6)
41+	17	(1/6)	0	(0/2)
Total	47	(33/70)	56	(29/52)

Table 3. *Number of households which showed intrafamilial spread of non-polio enterovirus, Ulaanbaatar and Tov province, Mongolia, late summer 2003*

Virus		No. of household(s) with intrafamilial spread/No. of household(s) with at least one infected individual
Group	Type	
Echo	30	8/10
	33	8/10
	12	0/1
	25	1/1
	Total different households*	16/20
Coxsackie	A10	1/7
	A2	0/1
	A4	0/1
	A24	0/1
	Total different households*	1/10
Total different households*		16/23

* There are households with multiple virus types; such households are counted as one.

In the 5 weeks of observation of 122 subjects, 69 non-polio enteroviruses were isolated (Table 1). Eight serotypes of non-polio enteroviruses (echovirus types 30, 33, 12, 25, coxsackie A10, A2, A4, and A24 variant) were isolated from 62 persons with an overall isolation rate of 51% (62/122). By neutralization, only echovirus 30 was identified; therefore, molecular typing was performed for the samples for which a virus serotype could not be identified by neutralization. By analysis of the VP1 region, molecular typing identified the serotypes of all samples, which included echovirus 12, 25, 33, coxsackie A2, A4, A10, and A24. Among the serotypes, echovirus 30 and 33 predominated: 21% (26/122) and 24% (29/122) of the subjects were shedding the respective viruses. In the 5-week period, six individuals yielded multiple virus types: one study child (age 5 months) excreted echovirus 30, 33, and coxsackie A10, one sibling (age 4 years) excreted echovirus 33 and coxsackie A4, one sibling (age 2 years) excreted echovirus 30 and coxsackie A10, and one study child (age 5 months) and two siblings (ages 2 and 4 years) excreted echovirus 33 and coxsackie A10. Overall the non-polio enterovirus isolation rate was highest among the 2–10 years age group (74%) (Table 1). 57% (17/30), 69% (18/26), 45% (13/29), 36% (8/22), 12·5% (1/8), and 71% (5/7) of study children, siblings, mothers, fathers, relatives, and contacts excreted non-polio enteroviruses.

Overall, 47% (33/70) of females and 56% (29/52) of males excreted non-polio enteroviruses (Table 2). Comparison between the two sexes indicated that there was a tendency for higher isolation rates among males in younger age groups and females in older age groups.

Detection of enterovirus on hands

No enterovirus was detected from any of the hand swabs of 46 subjects.

Familial spread of non-polio enterovirus

We determined intrafamilial spread through isolation of the same virus type with high sequence homology in the 5′NTR-VP4-VP2 region from two or more members in the same household. The number of households tested and households which showed intrafamilial spread of non-polio enterovirus are shown in Table 3. All isolates from members living in the same household had 100% sequence homology except two households from which sequences differed by one nucleotide. Intrafamilial spread was responsible for 54% (37/69) of non-polio enterovirus infections.

Out of 16 households in which intrafamilial spread was confirmed, mode of transmission within the household could be observed in nine households by the difference in timing of virus isolation among family members. It supports the view that siblings

Table 4. *Order of transmission of non-polio enterovirus within household determined by difference in timing of virus isolation, Ulaanbaatar and Tov province, Mongolia, late summer, 2003. Modes of transmission for the 16 households which showed intrafamilial spread are shown*

Household	Virus	Week 1	Week 2	Week 3	Week 4	Week 5
1	E30	S →	M			
2	E30	V S M C →	F			
3	E30		S →	V M		
4	E30		S →	V M F		
5	E30				V S →	M
6	E30	V M F				
7	E30	S C				
8	E33	V S M F →	C			
9	E33	V S M →	F			
10	E33		S →	V		
11	E33				V S →	M F C
12	E33	V S M F				
13	E33	V S F				
14	E33		S M			
15	E25			V S		
	E30			V S		
16	E33					V M
	CA 10	V S				

V, study child; S, sibling; M, mother, F, father; C, contact.

are chiefly responsible for introducing virus into the family (Table 4). Fifty-nine per cent (32/54) of intrafamilial contacts excreted virus when the sibling was excreting virus, whereas only 9% (2/23) excreted virus when the sibling was not excreting virus ($\chi^2_{DF=1}=14{\cdot}74$, $P<0{\cdot}001$ with Yates' correction; odds ratio 15·27, 95% confidence interval 3·25–71·86). Echoviruses were isolated from 62% (36/58) of people in contact with siblings excreting echovirus: 72% (13/18), 61% (11/18), 47% (7/15), 33% (1/3), and 100% (4/4) of study children, mothers, fathers, relatives, and contacts of siblings respectively excreted virus when the sibling excreted virus. Coxsackie A virus seemed to be self-limiting, among 15 people who came into contact with siblings shedding virus, only one infant (7%) excreted virus.

Factors associated with non-polio enterovirus infection

Factors associated with non-polio enterovirus isolation are shown in Tables 5 and 6. Factors associated with intrafamilial spread of non-polio enterovirus are shown in Table 7. Overall, crowding, water storage, cover on stored water, years of maternal and paternal education, type of water supply (well/water distribution service/piped water), and location of toilet (inside/outside/none) showed no influence on enterovirus isolation. However, for people living in houses, households with an inside toilet showed a significantly higher degree of intrafamilial spread compared to those with outside toilets (Table 7).

DISCUSSION

Limitation

Generalization should be made carefully for the following reasons: our results reflect non-polio enterovirus isolation under routine immunization of OPV, and interference may have occurred between polio and non-polio enterovirus, serological analysis on each serotype was not conducted, therefore, prior infection was not considered, enterovirus prevalence varies by year and by season, therefore the period of 5 weeks only provides a snapshot of the situation in Mongolia, a larger study population is required to assure generalizability, and a lack of throat swabs may have decreased the isolation rate as well as the detection of certain serotypes.

Impact of molecular typing

For non-poliovirus isolates, only echovirus 30 was identified through neutralization. The use of

Table 5. *Associations between demographic characteristics and non-polio enterovirus isolation, Ulaanbaatar and Tov province, Mongolia, late summer 2003*

Variables	No.	OR	95% CI
Age group (years)			
0–1	30	9·1	1·0–83·8
2–10	23	19·8	2·0–195·9
11–20	12	14·0	1·3–156·3
21–30	37	4·6	0·5–38·3
31–40	12	5·0	0·5–54·4
41+	8	1·0	
Family status			
Study child	30	9·1	1·0–83·8
Sibling	26	15·7	1·7–149·8
Mother	29	5·7	0·6–52·2
Father	22	4·0	0·4–38·6
Relative	8	1·0	
Area			
Ulaanbaatar slum area	49	7·9	2·9–21·6
Ulaanbaatar apartment area	32	1·6	0·6–4·3
Tov province	37	1·0	
Sex (age $\leqslant$10 years)			
Male	28	2·8	0·9–8·8
Female	25	1·0	
Sex (age $\geqslant$10 years)			
Male	24	0·6	0·2–1·8
Female	45	1·0	

OR, Odds ratio (calculated by univariate logistic regression); CI, confidence interval.

molecular typing in addition to neutralization allowed the identification of the serotypes of all samples including the coxsackie A group which is generally difficult to identify through neutralization. The effectiveness of the use of molecular typing to identify non-polio enteroviruses was confirmed in our study.

Isolation rate of non-polio enterovirus

Although there is difficulty in comparing data due to differences in specimens sampled, specimen sampling frequency, selection of subjects, and virus isolation and identification methods, the observed overall isolation rate of 51 and 64% among children under 10 years of age is by far the highest isolation rate reported. Previous studies conducted among young children in the United States [8] and Hungary [12] reported an isolation rate of 21 and 26% respectively, and an isolation rate of 61% was reported among children under 10 months of age in Ghana [13].

Enterovirus infections peak in the warm months and are least frequent in the cold months [23, 24]. The warm season in Mongolia is very short, and after the severe winter season, enterovirus infections may become extremely prevalent in the summer. Additionally, the sharp increase of tourists during the summer season, as well as the holding of Naadam, a national sports festival to which Mongolians gather from all over the country, in the beginning of July in Ulaanbaatar, may have created an environment which facilitated virus introduction as well as person-to-person transmission, therefore influencing the incidence of infection.

Age, sex and isolation rate of non-polio enterovirus

In our study, the 21–40 years age group showed a high isolation rate of 39%. Data on the isolation rate of non-polio enteroviruses among healthy adults is limited, and to our knowledge, this is the highest isolation rate reported among adults. Our study demonstrates that infection usually occurs in childhood, but asymptomatic infection can be remarkably high among adults, depending on previous infection history with a given serotype in a given locale.

Overall, more males were shedding non-polio enteroviruses than females. This supports the findings that enteroviral diseases occur more frequently in males [8, 25, 26] and indicates that the higher morbidity among males is due to a higher infection rate among males. However, although the sample size in the age groups was small, there appeared to be higher infection rate among females above age 11 years. This is consistent with a finding that there was predominance of female patients due to enteroviral disease in a group over the age of 10 years [8]. It has been suggested that biological reasons are responsible for the higher infection rate among males such as longer duration of virus excretion and higher virus titre in stools of males [27]. However, our finding of mother > father > relative infected within the same household suggests that higher infection rate among adult females may reflect higher contact frequency and intimacy with infected children.

OPV interference by non-polio enterovirus

A review of immunity among children in developing countries has indicated low rates of seroconversion